Performance Limits for Synthetic Aperture Radar – second edition

Armin W. Doerry

Sandia National Laboratories

Report Documentation Page

Public reporting burden for the collection of information is estimated to average 1 hour per response, including the time for reviewing instructions, searching existing data sources, gathering and maintaining the data needed, and completing and reviewing the collection of information. Send comments regarding this burden estimate or any other aspect of this collection of information, including suggestions for reducing this burden, to Washington Headquarters Services, Directorate for Information Operations and Reports, 1215 Jefferson Davis Highway, Suite 1204, Arlington VA 22202-4302. Respondents should be aware that notwithstanding any other provision of law, no person shall be subject to a penalty for failing to comply with a collection of information if it does not display a currently valid OMB control number.

1. REPORT DATE	2. REPORT TYPE	3. DATES COVERED
FEB 2006		**00-00-2006 to 00-00-2006**

4. TITLE AND SUBTITLE	5a. CONTRACT NUMBER
Performance Limits for Synthetic Aperture Radar - Second Edition	5b. GRANT NUMBER
	5c. PROGRAM ELEMENT NUMBER
6. AUTHOR(S)	5d. PROJECT NUMBER
	5e. TASK NUMBER
	5f. WORK UNIT NUMBER

7. PERFORMING ORGANIZATION NAME(S) AND ADDRESS(ES)	8. PERFORMING ORGANIZATION REPORT NUMBER
Sandia National Laboratories,Albuquerque ,NM	

9. SPONSORING/MONITORING AGENCY NAME(S) AND ADDRESS(ES)	10. SPONSOR/MONITOR'S ACRONYM(S)
	11. SPONSOR/MONITOR'S REPORT NUMBER(S)

12. DISTRIBUTION/AVAILABILITY STATEMENT
Approved for public release; distribution unlimited

13. SUPPLEMENTARY NOTES

14. ABSTRACT

15. SUBJECT TERMS

16. SECURITY CLASSIFICATION OF:			17. LIMITATION OF ABSTRACT	18. NUMBER OF PAGES	19a. NAME OF RESPONSIBLE PERSON
a. REPORT **unclassified**	b. ABSTRACT **unclassified**	c. THIS PAGE **unclassified**	**Same as Report (SAR)**	**70**	

Performance Limits for Synthetic Aperture Radar – second edition

Armin W. Doerry
SAR Applications Department

Sandia National Laboratories
PO Box 5800
Albuquerque, NM 87185-1330

ABSTRACT

The performance of a Synthetic Aperture Radar (SAR) system depends on a variety of factors, many which are interdependent in some manner. It is often difficult to 'get your arms around' the problem of ascertaining achievable performance limits, and yet those limits exist and are dictated by physics, no matter how bright the engineer tasked to generate a system design. This report identifies and explores those limits, and how they depend on hardware system parameters and environmental conditions. Ultimately, this leads to a characterization of parameters that offer optimum performance for the overall SAR system.

For example, there are definite optimum frequency bands that depend on weather conditions and range, and minimum radar PRF for a fixed real antenna aperture dimension is independent of frequency.

While the information herein is not new to the literature, its collection into a single report hopes to offer some value in reducing the 'seek time'.

ACKNOWLEDGEMENTS

CONTENTS

FOREWORD

Fundamental to the quality of a SAR image is its Signal to Noise Ratio (SNR). Noise is in fact error in the rendering of the imaged scene, and is due to a variety of phenomena from a variety of sources. The equation that evaluates SNR with respect to additive thermal noise is commonly called the Radar Equation. It is discussed in a multitude of texts and other references, but seldom with enough detail and background to fully appreciate the many nuances and parameter trades available to a system designer. Indeed, the various texts often make different simplifying assumptions along the way such that apparent inconsistencies exist between them.

An earlier report was written to address these problems and provide a detailed discussion of the Radar Equation.[1] As is inevitable with hindsight, however, an awareness manifested itself that additional and enhanced explanations were warranted in a number of areas, and some errors in the original report also needed to be corrected. This second edition attempts to do just this.

1 Introduction

Synthetic Aperture Radar (SAR) performance is dependent on a multitude of parameters, many of which are interrelated in non-linear fashions. Seemingly simple questions such as "What range can we operate at?", "What resolution can we get?", "How fast can we fly?", and "What frequency should we operate at?", are often (and rightly so) hesitantly answered with a slew of qualifiers (ifs, buts, givens, etc.).

These invariably result in performance studies that trade various parameters against each other. Nevertheless, general trends can be observed, and general statements can be made. Furthermore, performance bounds can be generated to offer first order estimates on the achievability of various performance goals. This report attempts to do just this.

2 The Radar Equation

The performance measure is Signal-to-Noise (energy) Ratio (SNR) in the SAR image. A brief recap on the development of this equation is as follows.

For a single pulse, the Received (RX) power at the antenna port is related to the Transmitted (TX) power by

$$P_r = P_t G_A \left(\frac{1}{4\pi R^2} \right) \sigma \left(\frac{1}{4\pi R^2} \right) A_e \left(\frac{1}{L_{radar} L_{atmos}} \right) = \frac{P_t G_A A_e \sigma}{(4\pi)^2 R^4 L_{radar} L_{atmos}} , \tag{1}$$

where

P_r = received signal power (W),

P_t = transmitter signal power (W),

G_A = transmitter antenna gain factor,

A_e = receiver antenna effective area (m^2),

σ = target Radar Cross Section (m^2),

R = range vector from target to antenna (m),

L_{atmos} = atmospheric loss factor due to the propagating wave,

L_{radar} = microwave transmission loss factor due to miscellaneous sources. (2)

The effective noise power that the signal must compete with at the antenna is given approximately by

$$N_r = kTF_N B_N , \tag{3}$$

where

N_r = received noise power (W),

k = Boltzmann's constant = 1.38 x 10-23 J/K,

T = nominal scene noise temperature $\approx$ 290 K,

F_N = system noise factor for the receiver,

B_N = noise bandwidth at the antenna port. (4)

Consequently, the Signal-to-Noise (power) ratio at the RX antenna port is effectively

$$SNR_{antenna} = \frac{P_r}{N_r} = \frac{P_t G_A A_e \sigma}{(4\pi)^2 R^4 L_{radar} L_{atmos} (kTF_N)B_N}.$$ (5)

A finite data collection time limits the total energy collected, and signal processing in the radar increases the SNR in the SAR image by two major gain factors. The fist is due to pulse compression, and the second is due to coherently combining echoes from multiple pulses. This results in

$$SNR_{image} = SNR_{antenna}G_r G_a = \frac{P_t G_A A_e \sigma \, G_r G_a}{(4\pi)^2 R^4 L_{radar} L_{atmos} (kTF_N)B_N},$$ (6)

where

G_r = SNR gain due to range processing (pulse compression),

G_a = SNR gain due to azimuth processing (coherent pulse integration). (7)

The product $G_r G_a$ comprise the signal processing gain.

This relationship is called "The Radar Equation".

At this point we examine the image SNR terms and factors individually to relate them to physical SAR system parameters and performance criteria.

2.1 Antenna

This report will consider only the monostatic case, where the same antenna is used for TX and RX operation. Consequently, we relate

$$G_A = \frac{4\pi A_e}{\lambda^2},$$ (8)

where λ is the nominal wavelength of the radar. Furthermore, the effective area is related to the actual aperture area by

$$A_e = \eta_{ap} A_A,$$ (9)

where

η_{ap} = the aperture efficiency of the antenna,

A_A = the physical area of the antenna aperture. (10)

Typically, a radar design must live with a finite volume for the antenna structure, so that the achievable antenna physical aperture area is limited. The aperture efficiency takes into account a number of individual efficiency factors, including the radiation efficiency of the antenna, the aperture illumination efficiency of say a feedhorn to a reflector assembly, spillover losses of a feedhorn to a finite reflector area, etc. A typical number for aperture efficiency might be $\eta_{ap} \approx 0.5$.

Putting these into the radar equation yields

$$SNR_{image} = \frac{P_t \left(\eta_{ap}^2 A_A^2 \right) \sigma \, G_r G_a}{(4\pi) R^4 \lambda^2 L_{radar} L_{atmos} \left(kTF_N \right) B_N} \, .$$ (11)

2.2 Processing gains

A detailed discussion of processing gain is given in Appendix A.

The range processing gain is due to noise bandwidth reduction during the course of pulse compression. It is straightforward to show that

$$G_r = \frac{T_{eff} B_N}{L_r} \, ,$$ (12)

where

T_{eff} = the effective pulse width of the radar, and

L_r = reduction in SNR gain due to non-ideal range filtering. (13)

Note that in the absence of more refined information, typically $L_r \approx a_{wr} \approx 1.2$ or so, where a_{wr} = the range impulse response broadening factor due to data weighting or windowing.

The effective pulse width differs from the actual TX pulse width in that the effective pulse width is equal to that portion of the real pulse that makes it into the data set. For digital matched-filter processing they are the same, but for stretch-processing the effective pulse width is typically slightly less than the real transmitted pulse width, but still pretty close. For the remainder of this report we will presume that the transmitted pulse width is equal to the effective pulse width.

The azimuth processing gain is due to the coherent integration of multiple pulses, whether by presumming or actual Doppler processing. Of course, the total number of pulses that can be collected depends on the radar Pulse Repetition Frequency (PRF) and the time it takes to fly the aperture, which in turn depends on platform velocity and the physical dimension of the synthetic aperture, which in turn depends on the azimuth resolution desired. Assuming a broadside collection geometry, and putting all this together yields

$$G_a = \frac{N}{L_a} = \frac{f_p \lambda R a_{wa}}{2 \rho_a v_x L_a},$$

(14)

where

N = the total number of pulses integrated,

f_p = radar PRF (Hz),

ρ_a = image azimuth resolution (m),

v_x = platform velocity (m/s), horizontal and orthogonal to the target direction,

a_{wa} = azimuth impulse response broadening factor,

L_a = reduction in SNR gain due to non-ideal azimuth filtering.

(15)

Note that in the absence of more refined information, typically $L_a \approx a_{wa} \approx 1.2$ or so.

Putting these into the radar equation yields

$$SNR_{image} = \frac{P_t T_{eff} f_p \left(\eta_{ap}^2 A_A^2 \right) \sigma a_{wa}}{2 (4\pi) v_x R^3 \lambda \rho_a \left(k T F_N \right) L_{radar} L_{atmos} L_r L_a}.$$

(16)

2.3 The Transmitter

The transmitter is generally specified to first order by 3 main criteria:

1) The frequency range of operation,

2) The peak power output (averaged during the pulse on-time), and

3) The maximum duty factor allowed.

We identify the duty factor as

$$d = T_{eff} f_p = \frac{P_{avg}}{P_t},$$

(17)

where P_{avg} is the average power transmitted during the synthetic aperture data collection period. Consequently, we identify

$$P_t T_{eff} f_p = P_t d = P_{avg} \, . \tag{18}$$

Transmitter power capabilities and bandwidths are very dependent on transmitter technology. In general, for tube-type power amplifiers, higher power generally implies lesser capable bandwidth, and hence lesser range resolution. The signal bandwidth required for a particular range resolution for a single pulse is given by

$$B_T = \frac{a_{wr} c}{2 \rho_r} \, , \tag{19}$$

where

ρ_r = slant-range resolution required,

a_{wr} = range impulse response broadening factor,

c = velocity of propagation. $\tag{20}$

There is no typical duty factor that characterizes all, or even most, power amplifiers. Duty factors may range from on the order of 1% to 100% across the variety of power amplifiers available. Typically, a maximum duty factor needed by a radar is less than 50%, and usually less than about 35% or so. Consequently, a reasonable duty factor limit of 35% might be imposed on power amplifiers that could otherwise be capable of more.

In practice, the duty factor limit for a particular power amplifier may not always be achieved due to timing constraints for the geometry within which the radar is operating, but we can often get pretty close.

We take this opportunity to also note that

$$\lambda = \frac{c}{f} \, , \tag{21}$$

where f is the radar nominal frequency.

2.3.1 Power Amplifier Tubes

The following table indicates some representative power amplifier tube capabilities.

Table 1. Power Amplifier Tubes.

Power Amplifier Tube	Frequency Band of Operation (GHz)	Peak Power (W)	Max Duty Factor	Avg Power (W)
CPI VTU-5010W2	15.2 - 18.2	320	0.35	112
Teledyne MEC 3086	15.5 - 17.9	700	0.35	245
Litton L5869-50	16.25 - 16.75	4000	0.30	1200
Teledyne MTI 3048D	8.7 - 10.5	4000	0.10	400
CPI VTX-5010E	7.5 - 10.5	350	0.35	123
Teledyne MTI3948R	8.7 - 10.5	7000	0.07	490
Litton L5806-50	9.0 - 9.8	9000	0.50	3150[a]
Litton L5901-50	9.6 - 10.2	20000	0.06	1200
Litton L5878-50	5.25 - 5.75	60000	0.035	2100
Teledyne MEC 3082	3.0 - 4.0	10000	0.04	400

2.3.2 Solid-State Amplifiers

Solid-state power amplifiers are generally lower in power than their tube counterparts, typically under 100 W, and more likely in the 10 W to 20 W range (depending on frequency band). However, they do offer a possible efficiency advantage, and technology is advancing to the point where these should be considered for relatively short range radar applications.

2.3.3 Electronic Phased-Arrays

An alternative to power amplifier tubes is an electronic Active Phased Array (APA), made up of many small, relatively low-power (generally solid-state) Transmit/Receive (T/R) modules. This is a scalable architecture that spatially combines the power from many individual elements. Current state-of-the-art is approaching 10 W of power from an X-band T/R module with 1 cm^2 cross section. This represents an aperture power density of 100 kW/ m^2. That is, heat dissipation problems notwithstanding, a rather small antenna aperture of 0.1 m^2 could possibly radiate 10 kW of peak power with a relatively high duty factor. New technologies such as GaN offer the promise of many tens of Watts at higher frequencies (Ku-band and even Ka-band) from a single MMIC. Furthermore, an

---

[a] based on 0.35 maximum duty factor.

Electronically Steerable Array (ESA) doesn't require a gimbal assembly for pointing, and could conceivably allow a larger broadside aperture area for a given antenna assembly volume constraint.

In any case, we refine the radar equation to be

$$SNR_{image} = \frac{P_{avg}\left(\eta_{ap}^2 A_A^2\right)f\ \sigma\ a_{wa}}{2(4\pi)cv_x R^3 \rho_a\left(kTF_N\right)L_{radar}L_{atmos}L_r L_a}\ ,\tag{22}$$

noting that the average power is based on the power amplifier's duty factor limit, or perhaps 35%, whichever is less.

2.4 The Target Radar Cross Section (RCS)

The RCS of a target denotes its ability to reflect energy back to the radar. For SAR, the target of interest in terms of radar performance is generally a distributed target, such as grass, corn fields, etc. For these target types, the RCS is dependent on the area being resolved. Consequently, for distributed targets, RCS is generally specified as a reflectivity number that normalizes RCS per unit area. The actual area is the area of a resolution cell, as projected on the ground. Consequently

$$\sigma = \sigma_0 \rho_a \rho_y = \sigma_0 \rho_a \left(\frac{\rho_r}{\cos\psi_g}\right),\tag{23}$$

where

σ_0 = distributed target reflectivity (m^2/m^2),

ρ_y = range resolution in the ground-plane,

ψ_g = grazing angle at the target location. $\tag{24}$

In addition, σ_0 is generally frequency-dependent, typically proportional to f^n, where n depends on target type, with $0 < n < 1$, but usually closer to one.[2] Consequently we can write

$$\sigma = \sigma_{0,ref}\left(\frac{\rho_a \rho_r}{\cos\psi_g}\right)\left(\frac{f}{f_{ref}}\right)^n,\tag{25}$$

where $\sigma_{0,ref}$ is the reflectivity of interest at nominal reference frequency f_{ref}. At this point, target RCS embodies a frequency dependence, as it should.

We note that even for non-distributed targets, a variety of frequency dependencies exists, and are characterized in the following table.

Table 2. RCS frequency dependence.

target characteristic	examples	frequency dependence
2 radii of curvature	spheroids	none
1 radius of curvature	cylinders, top hats	f
0 radii of curvature	flat plates, dihedrals, trihedrals	f^2

A typical radar specification requires a SNR of 0 dB for a target reflectivity of –25 dB at Ku-band (nominally 16.7 GHz). This corresponds to $\sigma_{0,ref} = -25$ dB, with $f_{ref} = 16.7$ GHz. The implication is that the same target scene would be dimmer at lower frequencies, and brighter at higher frequencies.

Additionally, $\sigma_{0,ref}$ will exhibit some dependency itself on grazing angle ψ_g. This dependency is sometimes incorporated into a model known as 'constant-γ' reflectivity model. Other times the grazing angle dependence is just ignored.

Nevertheless, folding the RCS dependencies into the radar equation, and rearranging a bit, yields

$$SNR_{image} = \frac{P_{avg}\left(\eta_{ap}^2 A_A^2\right)\rho_r \sigma_{0,ref}\left(\dfrac{f}{f_{ref}}\right)^n f \, a_{wa}}{(8\pi)cv_x R^3 \cos\psi_g \left(kTF_N\right)L_{radar}L_{atmos}L_r L_a}. \tag{26}$$

2.5 Radar Geometry

Typically, the radar is specified to operate at a particular height. Consequently, grazing angle depends on this height and the slant-range of operation. That is, for a flat earth,

$$\sin\psi_g = \frac{h}{R}, \tag{27}$$

or

$$\cos\psi_g = \sqrt{1-\left(\frac{h}{R}\right)^2}, \tag{28}$$

where h = the height of the radar above the target.

This yields a radar equation as follows,

$$SNR_{image} = \frac{P_{avg}\left(\eta_{ap}^2 A_A^2\right)\rho_r \sigma_{0,ref}\left(\dfrac{f}{f_{ref}}\right)^n f\, a_{wa}}{(8\pi)cv_x R^3 \sqrt{1-\left(\dfrac{h}{R}\right)^2}\left(kTF_N\right)L_{radar}L_{atmos}L_r L_a}\,. \tag{29}$$

2.6 SNR Losses and Noise Factor

The radar equation as presented notes several broad categories of SNR losses.

2.6.1 Signal Processing Losses

These include the SNR loss (relative to ideal processing gains) due to employing a window function. Recall that the window bandwidth (including its noise bandwidth) is increased somewhat. If window functions are incorporated in both dimensions (range and azimuth processing), then we incur a SNR loss typically slightly larger than the impulse response broadening factor, perhaps on the order of 1 dB for each dimension.

If a target of interest is other than distributed, we might also incorporate an additional 'straddling' loss due to a target not being centered in a resolution cell. This depends on the relationship of pixel spacing to resolution, also known as the oversampling factor, but might be as high as 3 dB. For distributed targets, being off-center of a resolution cell is meaningless.

2.6.2 Radar Losses

These include a variety of losses primarily over the microwave signal path, but doesn't include the atmosphere. Included are a power loss from transmitter power amplifier output to the antenna port, and a two-way loss through the radome. These are generally somewhat frequency dependent, being higher at higher frequencies, but major effort is expended to keep them both as low as is reasonably achievable. In the absence of more refined information, typical numbers might be 0.5 dB to 2 dB from TX amplifier to the antenna port, and perhaps an additional 0.5 dB to 1.5 dB two-way through the radome.

2.6.3 System Noise Factor

When this number is expressed in dB, it is often referred to as the system noise figure.

The system noise figure includes primarily the noise figure of the front-end Low-Noise Amplifier (LNA) and the losses between the antenna and the LNA. These both are a function of a variety of factors, including the length and nature of cables required, LNA protection and isolation requirements, and of course frequency. Frequency dependence is generally such that higher frequencies will result in higher system noise figures. For example, typical system noise figures for sub-kilowatt radar systems are 3.0 dB to 3.5 dB at X-band, 3.5 dB to 4.5 dB at Ku-band, and perhaps 6 dB at Ka-band.

2.6.4 Atmospheric Losses

Atmospheric losses depend strongly on frequency, range, and the nature of the atmosphere (particularly the weather conditions) between radar and target. Major atmospheric loss factors are atmospheric density, humidity, cloud water content, and rainfall rate. These conspire to yield a 'loss-rate' often expressed as dB per unit distance, that is very altitude and frequency dependent. The loss-rate generally increases strongly with frequency, but decreases with radar altitude, owing to the signal path traversing a thinner average atmosphere.

A typical radar specification is to yield adequate performance in an atmosphere that includes weather conditions supporting a 4 mm/Hr rainfall rate on the ground.

We identify the overall atmospheric loss as

$$L_{atmos} = 10^{\frac{\alpha R}{10}}, \tag{30}$$

where α = the two-way atmospheric loss rate in dB per unit distance.

Nominal two-way loss rates from various altitudes for some surface rain rates are listed in the following tables. While numbers listed are to several significant digits, these are based on a model and are quite squishy.[3,4]

Incorporating atmospheric loss-rate overtly into the radar equation, and rearranging a bit, yields

$$SNR_{image} = \frac{P_{avg}\left(\eta_{ap}^2 A_A^2\right)\rho_r \sigma_{0,ref}\left(\dfrac{f}{f_{ref}}\right)^n f \ a_{wa}}{(8\pi)cv_x\left(kTF_N\right)\left(L_{radar}L_r L_a\right)\left(R^3\sqrt{1-\left(\dfrac{h}{R}\right)^2} \ 10^{\frac{\alpha R}{10}}\right)}. \tag{31}$$

Implicit in the radar equation is that atmospheric loss-rate a depends on f in a decidedly nonlinear manner (and not necessarily even monotonic near specific absorption bands - of note are an H_2O absorption band at about 23 GHz, and an O_2 absorption band at about 60 GHz).

Table 3. Two-way loss rates (dB/km) in 50% RH clear air.

Radar Altitude (kft)	L-band 1.5 GHz	S-band 3.0 GHz	C-band 5.0 GHz	X-band 9.6 GHz	Ku-band 16.7 GHz	Ka-band 35 GHz	W-band 94 GHz
5	0.0119	0.0138	0.0169	0.0235	0.0648	0.1350	0.7101
10	0.0110	0.0126	0.0149	0.0197	0.0498	0.1053	0.5357
15	0.0102	0.0115	0.0133	0.0170	0.0400	0.0857	0.4236
20	0.0095	0.0105	0.0120	0.0149	0.0333	0.0721	0.3476
25	0.0087	0.0096	0.0108	0.0132	0.0282	0.0616	0.2907
30	0.0080	0.0088	0.0099	0.0119	0.0246	0.0541	0.2515
35	0.0074	0.0081	0.0090	0.0108	0.0218	0.0481	0.2214
40	0.0069	0.0075	0.0083	0.0099	0.0196	0.0434	0.1977
45	0.0064	0.0069	0.0076	0.0090	0.0176	0.0392	0.1774
50	0.0059	0.0064	0.0071	0.0083	0.0161	0.0360	0.1617

Table 4. Two-way loss rates (dB/km) in 4 mm/Hr (moderate) rainy weather.

Radar Altitude (kft)	L-band 1.5 GHz	S-band 3.0 GHz	C-band 5.0 GHz	X-band 9.6 GHz	Ku-band 16.7 GHz	Ka-band 35 GHz	W-band 94 GHz
5	0.0135	0.0207	0.0502	0.1315	0.5176	2.1818	8.7812
10	0.0126	0.0193	0.0450	0.1107	0.4062	1.7076	7.7623
15	0.0117	0.0175	0.0391	0.0920	0.3212	1.3311	6.4537
20	0.0106	0.0150	0.0314	0.0714	0.2453	1.0082	4.8836
25	0.0096	0.0132	0.0264	0.0584	0.1979	0.8108	3.9218
30	0.0088	0.0118	0.0228	0.0496	0.1662	0.6788	3.2796
35	0.0081	0.0107	0.0201	0.0431	0.1433	0.5838	2.8178
40	0.0074	0.0098	0.0180	0.0382	0.1259	0.5122	2.4701
45	0.0069	0.0089	0.0163	0.0342	0.1121	0.4558	2.1967
50	0.0064	0.0082	0.0149	0.0310	0.1012	0.4109	1.9793

Table 5. Two-way loss rates (dB/km) in 16 mm/Hr (heavy) rainy weather.

Radar Altitude (kft)	L-band 1.5 GHz	S-band 3.0 GHz	C-band 5.0 GHz	X-band 9.6 GHz	Ku-band 16.7 GHz	Ka-band 35 GHz	W-band 94 GHz
5	0.0166	0.0373	0.1531	0.4910	1.8857	7.3767	23.0221
10	0.0159	0.0347	0.1282	0.3829	1.4091	5.6330	21.0363
15	0.0146	0.0307	0.1060	0.3020	1.0738	4.3037	17.7448
20	0.0128	0.0249	0.0816	0.2289	0.8097	3.2377	13.3520
25	0.0113	0.0211	0.0665	0.1844	0.6459	2.5944	10.6964
30	0.0102	0.0184	0.0563	0.1546	0.5425	2.1651	8.9251
35	0.0093	0.0163	0.0488	0.1331	0.4658	1.8578	7.6569
40	0.0085	0.0147	0.0431	0.1169	0.4081	1.6269	6.7043
45	0.0078	0.0133	0.0386	0.1042	0.3630	1.4467	5.9604
50	0.0073	0.0122	0.0349	0.0940	0.3270	1.3027	5.3667

2.7 Other Useful Expressions and Observations

The radar equation comes in a plethora of versions based on different parameters. We begin with

$$SNR_{image} = \frac{P_{avg}\left(\eta_{ap}^2 A_A^2\right)\rho_r \sigma_{0,ref}\left(\dfrac{f}{f_{ref}}\right)^n f\, a_{wa}}{(8\pi)cv_x\left(kTF_N\right)\left(L_{radar}L_r L_a\right)\left(R^3\sqrt{1-\left(\dfrac{h}{R}\right)^2}\,10^{\frac{\alpha R}{10}}\right)} \tag{32}$$

Another useful expression is

$$SNR_{image} = \left(\frac{P_{avg}G_A^2\lambda^3\rho_y\sigma_{0,ref}}{2(4\pi)^3 R^3 v_x\left(kTF_N\right)a_{wr}}\right)\left(\frac{1}{L_{radar}10^{\frac{\alpha R}{10}}}\right)\left[\frac{a_{wr}a_{wa}}{L_r L_a}\right]\left[\frac{f}{f_{ref}}\right]^n. \tag{33}$$

Some useful observations include

- SNR does not depend on azimuth resolution.

- PRF can be traded for pulse width to keep P_{avg} constant.

- For constant ground-range resolution, there is no SNR overt dependence on grazing angle, although $\sigma_{0,ref}$ itself may exhibit some dependence on grazing angle as previously discussed, and atmospheric loss depends on height and range.

- Input Noise bandwidth B_N has no direct effect on ultimate image SNR. Signal bandwidth does not explicitly impact SNR directly, but rather through a looser dependence of ρ_y and perhaps L_r.

- The expressions in the square brackets are typically nearly unity, or at least often presumed to be so, and so are often ignored. If so, then the processing losses should not be double counted elsewhere.

Appendix B discusses other forms for the SAR Radar Equation as presented in several other texts.

2.8 Grouping Parameters due to Geometry, Hardware, and Processing

Influential parameters can be divided into three principal categories, namely

1. Radar operating geometry and environment,
2. Radar hardware limitations, and
3. Radar signal processing.

We now examine the radar equation with respect to these categories. The Radar Equation in the previous development can easily be manipulated to be

$$SNR_{image} = \frac{P_{avg} G_A{}^2 \lambda^3 \sigma_0 \rho_r a_{wa}}{2(4\pi)^3 R^3 v_x \cos\psi_g (kTF_N) L_{radar} L_{atmos} L_r L_a}. \tag{34}$$

Rather than specifying the image SNR with respect to some target scene reflectivity, the radar equation for SAR is more often written in a manner that assumes that image SNR is unity for some noise equivalent scene reflectivity. Indeed, the achievable noise equivalent reflectivity can be calculated as

$$\sigma_N = \frac{\sigma_0}{SNR_{image}} = \frac{2(4\pi)^3 R^3 v_x \cos\psi_g (kTF_N) L_{radar} L_{atmos} L_r L_a}{P_{avg} G_A{}^2 \lambda^3 \rho_r a_{wa}}. \tag{35}$$

To facilitate the subsequent discussion, we make use of

$$\rho_r = a_{wr} \frac{c}{2B_T} \tag{36}$$

where B_T = the effective signal bandwidth of the radar waveform within the data, and rewrite the equivalent reflectivity with parameters grouped as

$$\sigma_N = \frac{256\pi^3 kT}{c} \left(R^3 v_x \cos\psi_g\right) \left(\frac{B_T F_N L_{radar} L_{atmos}}{P_{avg} G_A{}^2 \lambda^3}\right) \left(\frac{L_r L_a}{a_{wr} a_{wa}}\right). \tag{37}$$

The parameters preceding the parentheses are constants that will not be discussed any further.

Radar operating geometry and environment

The first set of parameters $\left(R^3 v_x \cos\psi_g\right)$ deal with the radar platform's physical relationship with respect to the target scene. These include where the radar is, where it is

going, and how fast it is getting there. These parameters are important to the radar designer as they certainly impact the needed functionality of the hardware design, but otherwise are not controllable by the radar hardware designer.

The nominal geometry is specified by R and ψ_g. The radar platform's motion is specified by v_x.

Radar hardware limitations

The second set of parameters $\left(B_T F_N L_{radar} L_{atmos}\right)\big/\left(P_{avg} G_A{}^2 \lambda^3\right)$ deal with radar hardware limitations. These need to be selected by a hardware designer based on the limitations of radar geometry and environment, but mindful of the needs of the radar signal processing. The purpose of the hardware is to provide usable data to the signal processor, but otherwise cannot control how the signal processor chooses to specifically process the data into an image.

Radar wavelength λ is a fundamental parameter of the hardware. The antenna gain G_A is normally fixed by its construction. The transmitter is limited by its hardware to some maximum P_{avg}, although it may be specified via a maximum peak transmitter power with some maximum duty factor. The radar duty factor, in turn, is proportional to both radar PRF and pulse width. Some radar geometries may affect allowable duty factors and hence P_{avg}, but achievable P_{avg} under these circumstances is still a radar hardware design limitation. The effective signal bandwidth B_T is nominally the transmitted signal bandwidth, but may perhaps be limited by receiver bandwidth. The receiver will also exhibit some noise figure F_N that is a function of its construction.

Hardware system losses are embodied in L_{radar}. The atmospheric propagation loss L_{atmos} is a function of geometry, but is also a function of the radar operating wavelength λ. More commonly, a weather model is specified for the radar that is wavelength independent (e.g. clear air, or must accommodate 4 mm/Hr rain, etc.) When a weather model is specified, in addition to the geometry, then the radar designer does have some control over the specific value for L_{atmos} via selecting the radar wavelength.

The effective signal bandwidth B_T will impose limitations on ultimate achievable range resolution ρ_r, although precise values of range resolution depend on radar signal processing.

Radar signal processing

The third set of parameters $\left(L_r L_a\right)\big/\left(a_{wr} a_{wa}\right)$ deal with signal processing issues in the image formation processor. Fundamental limits exist within the data on achievable resolution and ultimately σ_N. These can, of course, always be made worse with signal processing, but not better than the hardware-limited data can support. Practical

superresolution for this purpose (bandwidth extrapolation of an arbitrary scene) has been discredited.[5]

The nature of range sidelobe filtering will coarsen range resolution by the factor a_{wr}, and reduce the range processing gain with respect to ideal matched filtering by a factor L_r. Similarly, the nature of azimuth sidelobe filtering will coarsen azimuth resolution by the factor a_{wa}, and reduce the azimuth processing gain with respect to ideal matched filtering by a factor L_a.

3 Performance Issues

What follows is a discussion of several issues impacting performance of a SAR.

3.1 Optimum Frequency

For this report, the optimum frequency band of operation is that which yields the maximum SNR in the image for the targets of interest.

For constant average transmit power, constant antenna aperture, constant resolution, constant velocity, and constant system losses, the SNR in the image is proportional to

$$SNR_{image} \propto f^{(n+1)}10^{\frac{-\alpha R}{10}} , \tag{38}$$

where atmospheric loss rate α also depends on frequency (generally increasing with frequency as previously discussed). Clearly, for any particular range R, some optimum frequency exists to yield a maximum SNR in the image.

Figures 1 through 5 indicate the relative SNR in the image as a function of slant-range for various frequency bands.
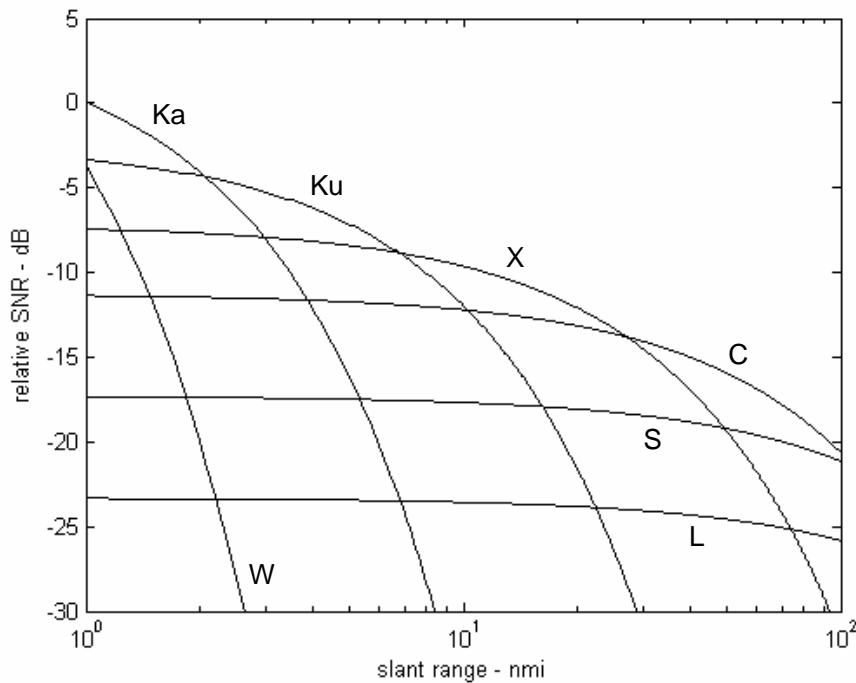
Figure 1. SAR relative performance of radar bands as a function of range (4 mm/Hr rain, 5 kft altitude, n=1).
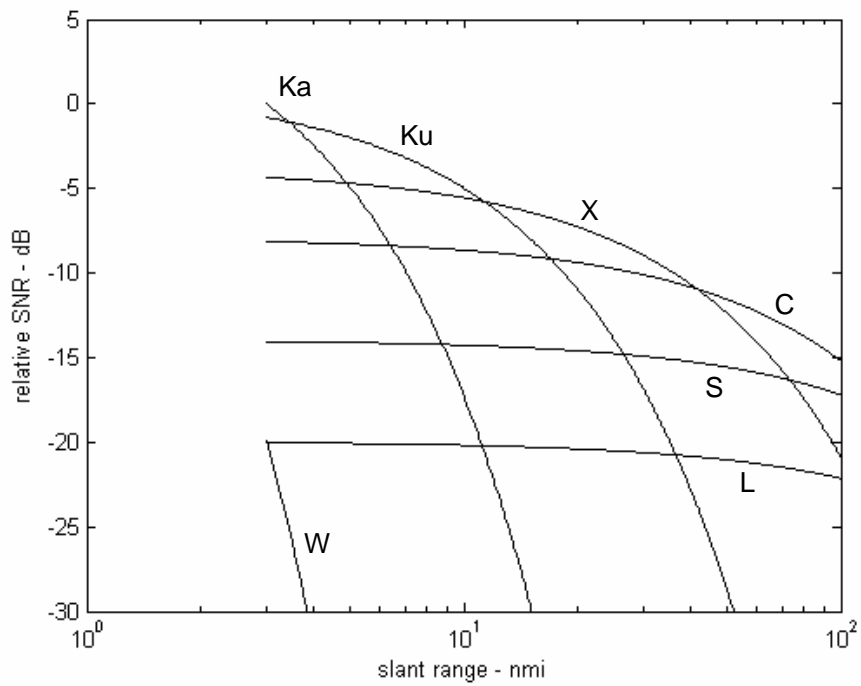
**Figure 2. SAR relative performance of radar bands as a function of range
(4 mm/Hr rain, 15 kft altitude, n=1).**
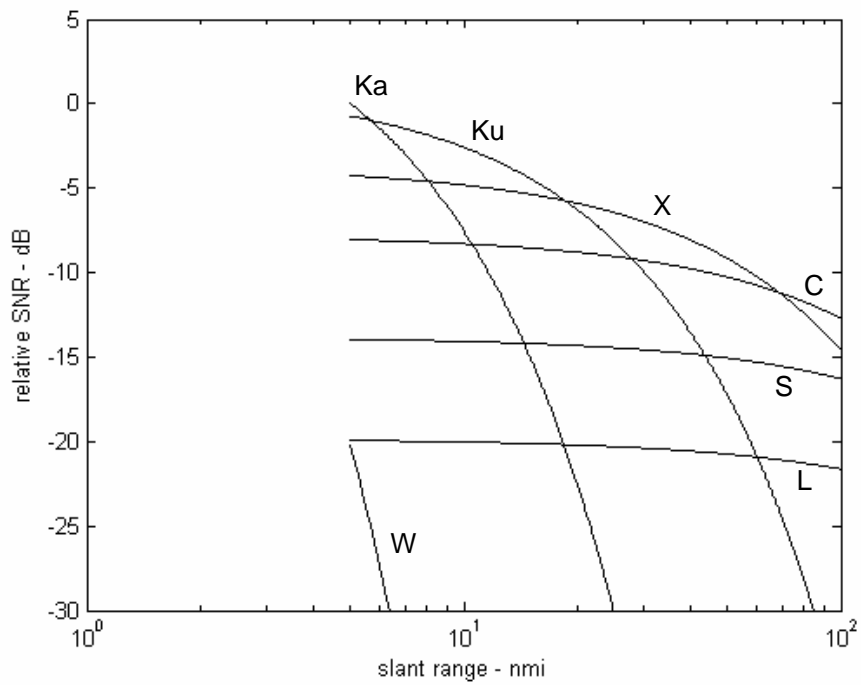
**Figure 3. SAR relative performance of radar bands as a function of range
(4 mm/Hr rain, 25 kft altitude, n=1).**
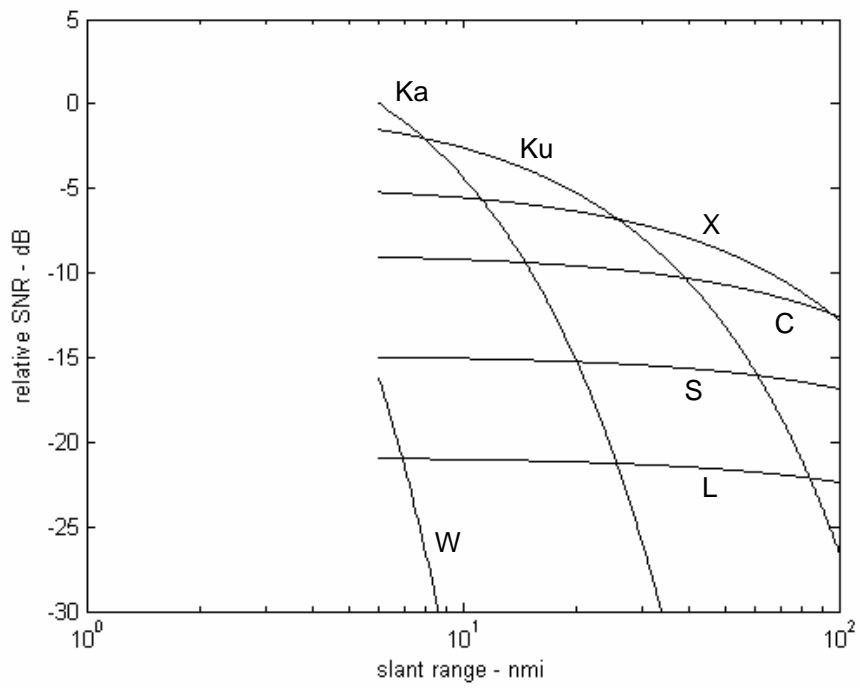
Figure 4. SAR relative performance of radar bands as a function of range (4 mm/Hr rain, 35 kft altitude, n=1).
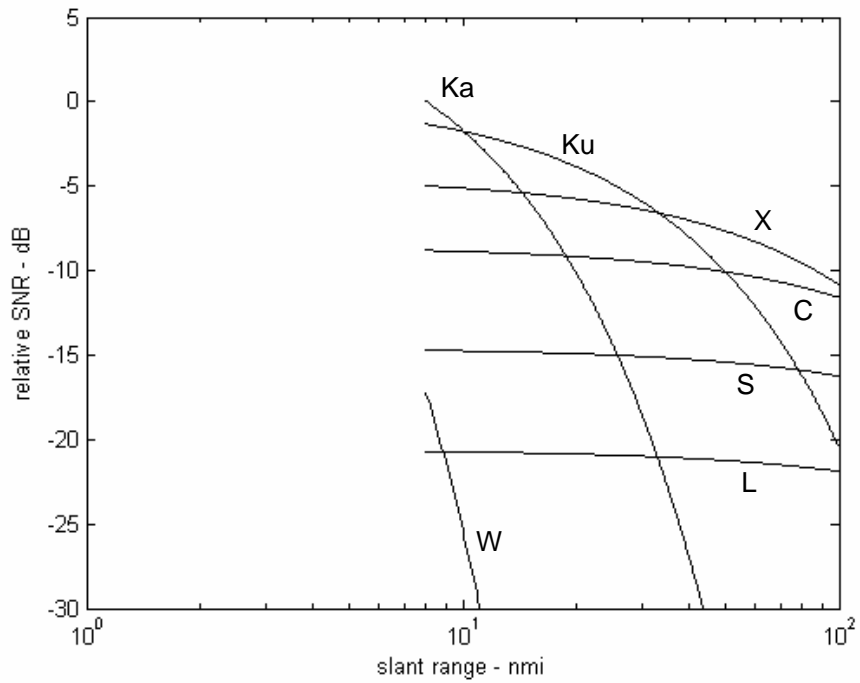
Figure 5. SAR relative performance of radar bands as a function of range (4 mm/Hr rain, 45 kft altitude, n=1).

In summary, for a constant real antenna aperture size, antenna gain increases with frequency, as does brightness of the target. However, as range increases, atmospheric losses increase correspondingly and more so at higher frequencies, eventually overcoming any advantage due to antenna gain and target brightness. Consequently, for any particular atmosphere, radar height and range, there exists an optimum frequency band for SAR operation.

Generally, as range increases and/or weather gets worse, lower frequencies become more attractive.

Optimal frequencies for a typical SAR weather specification are illustrated in figure 6.
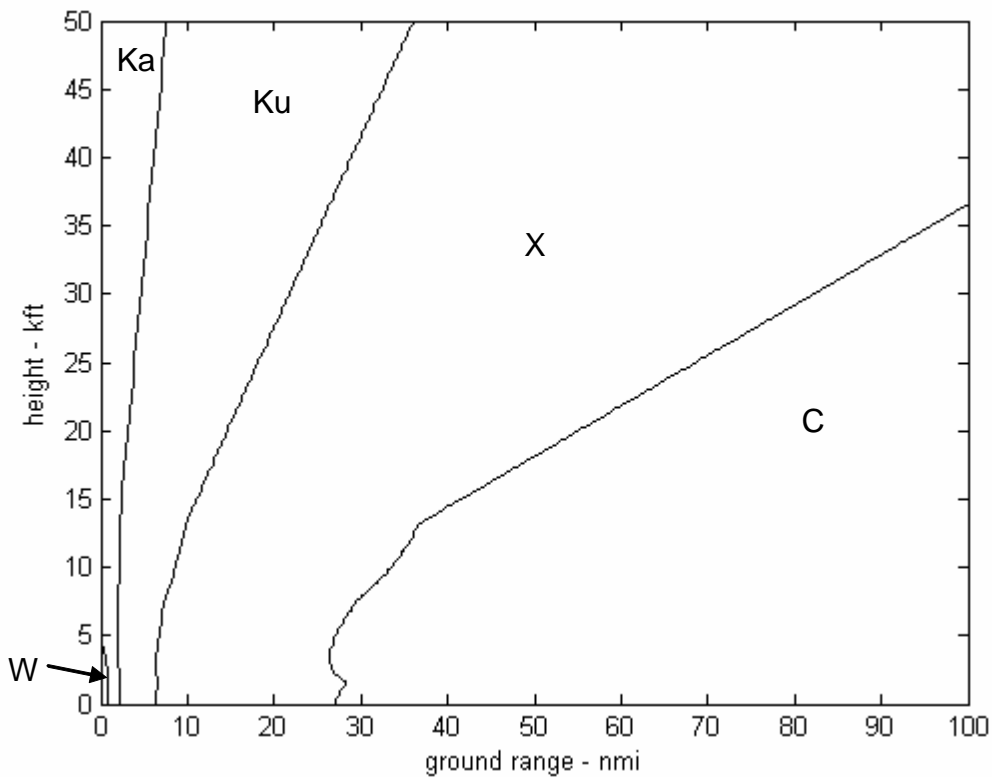
Figure 6. Optimum radar band as a function of range and altitude
(4mm/Hr rain, n=1, constant antenna aperture area).

It should be noted that other reasons (besides optimal SNR) may exist for choosing a particular radar band for operation (e.g. spectral compatibility, pre-existing hardware, hardware availability, ATR template compatibility, program directive, etc.).

3.2 PRF vs. Frequency

The Doppler bandwidth of a static scene is constrained by the antenna beamwidth to be

$$B_{Doppler} \approx \frac{2}{\lambda} v_x \theta_{az} \tag{39}$$

where θ_{az} = antenna azimuth beamwidth (presumed to be small).

The radar PRF is then chosen to be greater than this by some constant factor k_a, to limit aliasing, thereby yielding

$$f_p = k_a B_{Doppler} . \tag{40}$$

Typically, $k_a \geq 1.5$ or so, to account for the antenna beam roll-off. Actual minimum values will depend on the actual antenna pattern and allowable aliasing levels.

Noting that the antenna beamwidth is related to its physical aperture dimension D_{az} by

$$\theta_{az} \approx \frac{\lambda}{D_{az}} \tag{41}$$

yields the overall expression for PRF as

$$f_p \approx \frac{2k_a v_x}{D_{az}} . \tag{42}$$

The interesting feature of this expression is that the radar PRF depends on the ratio of velocity to aperture dimension of the real antenna, but not on the radar wavelength. Consequently, for a fixed aperture size and velocity, the PRF is independent of frequency.

We note that Equation (41) is an approximate relationship between aperture dimension and beamwidth. A more precise relationship would depend on the actual aperture illumination characteristic, and probably yields a somewhat broader beam. Nevertheless, the underlying truth is that though Doppler is inversely proportional to wavelength, antenna beamwidth tends to be directly proportional to wavelength. Since these are multiplied to yield the total Doppler bandwidth observed in the antenna beam, they cancel in a manner to hold the total Doppler bandwidth constant over wavelength, thereby allowing a PRF independent of wavelength, as indicated in Equation (42).

3.3 Signal to Clutter in rain

While noise can obfuscate the SAR image, so too can competing echoes from undesired sources such as rain. Rain falling in the vicinity of a target scene will 'clutter' the image of that scene. For this analysis we identify the Signal-to-Clutter Ratio (SCR) as the ratio of signal energy (echo energy from a resolution cell of the target scene) to the clutter energy (echo energy from the rain processed into the same resolution cell of the target scene).

Raindrops are generally small with respect to a wavelength and nearly spherical, indicating Rayleigh scattering, but there are a whole lot of them. The volume reflectivity (RCS per unit volume) of rain is modeled by[6]

$$\sigma_V = \left(7 \times 10^{-12}\right) r^{1.6} f_{GHz}^4 \quad \text{m}^2/\text{m}^3 \tag{43}$$

where

r = rain rate in mm/Hr,
f_{GHz} = frequency in GHz. $\tag{44}$

This model agrees with measured data pretty well up to about Ka-band.[7] Tabulated values from this model are given in the following table.

Table 6. Rain volume reflectivity (dBm^{-1}) vs. rain rates.

Rain Rate mm/Hr	L-band 1.5 GHz	S-band 3.0 GHz	C-band 5.0 GHz	X-band 9.6 GHz	Ku-band 16.7 GHz	Ka-band 35 GHz
0.25	−114	−102	−93	−82	−72	−59
1	−105	−92	−84	−72	−63	−50
4	−95	−83	−74	−63	−53	−40
16	−85	−73	−64	−53	−43	−31

Additionally, rain is not a static target, and exhibits its own motion spectrum. The motion spectrum typically is centered at some velocity with a recognizable velocity bandwidth. Data suggests a velocity bandwidth sometimes as high as 8 m/s, with a median velocity bandwidth of about 4 m/s.[8]

The RCS of a single resolution cell from the scene of interest is identified again as

$$\sigma_{target} = \frac{\sigma_{0,ref} \rho_a \rho_r}{\cos \psi_g} \left(\frac{f}{f_{ref}} \right)^n . \tag{45}$$

Correspondingly, the RCS of rain in a volume defined by the radar's resolution is

$$\sigma_{rain} = \sigma_V \rho_a \rho_r \rho_e$$

where ρ_e = elevation resolution (limited by extent of rain height).

We identify the elevation resolution as

$$\rho_e = \min\left(\frac{R\sin\theta_{el}}{2}, \frac{h_r}{\cos\psi_g} \right) \tag{46}$$

where

θ_{el} = elevation beamwidth of the antenna, and

h_r = height extent of rain (typically 3 to 4 km). (47)

The factor "2" in equation (46) accounts for the beam being aimed at the ground, and only half the beam intersecting the rain above ground for the resolution cell of interest.

If the rain were static, that is, not moving at all, then the volume of rain would be completely coherent, as is the target resolution cell. In this case, the SCR due to rain is

$$SCR_{rain} = \frac{\sigma_{target}}{\sigma_{rain}} . \tag{48}$$

If the rain were completely noncoherent, then the rain response would not benefit from any coherent processing gain, much like thermal noise. In this case the SCR due to rain is increased to

$$SCR_{rain} = \frac{\sigma_{target}}{(1/N)\sigma_{rain}} . \tag{49}$$

In reality, rain is typically somewhere in-between completely coherent over an entire synthetic aperture, and completely non-coherent from pulse to pulse. Consequently we define C as the coherency factor for rain, and identify

$$SCR_{rain} = \frac{\sigma_{target}}{C\sigma_{rain}} . \tag{50}$$

The rain coherency factor addresses the extent to which rain is coherent over the aperture collection time. If the rain is a coherent phenomena, then $C = 1$. If the rain is completely noncoherent, then $C = 1/N$. In fact, rain is somewhere in-between completely and forever coherent, and completely noncoherent. We identify the rain coherency interval (time) as the inverse of the rain Doppler frequency bandwidth, which in turn depends on the rain's velocity bandwidth. Consequently, we identify

$$C = \frac{T_{rain\_coherence}}{T_a} = \frac{f_p}{N\left(\frac{2}{\lambda}B_{rain\_velocity}\right)} \tag{51}$$

where

$1/N \leq C \leq 1$,

$T_{rain\_coherence}$ = rain coherence interval = $\left(\frac{2}{\lambda}B_{rain\_velocity}\right)^{-1}$,

$B_{rain\_velocity}$ = velocity bandwidth of rain in m/s, and

T_a = aperture collection interval = N/f_p . $\tag{52}$

We note that for $C=1$, the rain is coherent and any single column of rain falls into a single resolution cell. For $C = 1/N$, the rain is completely noncoherent and any single column of rain is smeared across all resolution cells.

Combining all the results yields

$$SCR_{rain} = \frac{\sigma_{target}}{C\sigma_{rain}} = \left(\frac{\sigma_{0,ref}\left(\frac{f}{f_{ref}}\right)^n}{\sigma_V}\right)\left(\frac{N\left(\frac{2}{\lambda}B_{rain\_velocity}\right)}{f_p\rho_e\cos\psi_g}\right). \tag{53}$$

If we also assume ρ_e is limited by the antenna beam, and that

$$\sin\theta_{el} \approx \theta_{el} \approx \frac{\lambda}{D_{el}} \tag{54}$$

where D_{el} is the antenna elevation aperture dimension, then

$$SCR_{rain} = \left(\frac{\sigma_{0,ref}}{\sigma_V}\right)\left(\frac{f}{f_{ref}}\right)^n\left(\frac{4ND_{el}B_{rain\_velocity}}{\lambda^2 f_p R\cos\psi_g}\right) = \left(\frac{\sigma_{0,ref}}{\sigma_V}\right)\left(\frac{f}{f_{ref}}\right)^n\left(\frac{2a_{wa}D_{el}B_{rain\_velocity}}{\rho_a\lambda v_x\cos\psi_g}\right) \tag{55}$$

or, plugging in the rain volume reflectivity

$$SCR_{rain} = \sigma_{0,ref}\left(\frac{f}{f_{ref}}\right)^n\left(\frac{2}{7\times10^{-48}}\right)\left(\frac{a_{wa}D_{el}B_{rain\_velocity}}{r^{1.6}f^3\rho_a cv_x\cos\psi_g}\right). \tag{56}$$

Clearly, SCR due to rain gets worse at higher frequencies, heavier rain rates, coarser resolutions, and higher platform velocities. Just how bad is it? The following tables quantify some SCRs.

Table 7. SCR_{rain} **(dB) for 1 m resolution at** v_x **= 50 m/s,**
($\sigma_{0,ref}$ = −25 dB at f_{ref} **= 16.7 GHz,** D_{el} **= 0.2 m,** $B_{rain\_velocity}$ **= 4 m/s,** a_{wa}**=1.2,** ψ_g**=30 deg.)**

Rain Rate mm/Hr	L-band 1.5 GHz	S-band 3.0 GHz	C-band 5.0 GHz	X-band 9.6 GHz	Ku-band 16.7 GHz	Ka-band 35 GHz
0.25	72	66	62	56	51	45
1	62	56	52	46	42	35
4	53	47	42	37	32	26
16	43	37	33	27	22	16

Table 8. SCRrain (dB) for 10 m resolution at v_x **= 280 m/s**
($\sigma_{0,ref}$ = −25 dB at f_{ref} **= 16.7 GHz,** D_{el} **= 0.2 m,** $B_{rain\_velocity}$ **= 4 m/s,** a_{wa}**=1.2,** ψ_g**=30 deg.)**

Rain Rate mm/Hr	L-band 1.5 GHz	S-band 3.0 GHz	C-band 5.0 GHz	X-band 9.6 GHz	Ku-band 16.7 GHz	Ka-band 35 GHz
0.25	55	49	44	39	34	27
1	45	39	35	29	24	18
4	35	29	25	19	14	8.0
16	26	20	15	9.6	4.8	−1.6

Since a typical SAR noise specification in the image is equivalent to a target scene reflectivity of −25 dB at Ku-band, we note from the tables that we expect rain to be noticeable only for the worst rain rates, at the highest frequencies, at extremely coarse resolutions, and at substantial velocities. Nevertheless, while most airborne SARs do not, some SARs do in fact operate under these conditions which warrants a cursory check of rain clutter sensitivity. After all, radar is touted as an all/adverse-weather sensor.

3.4 Pulses in the Air

Typical operation for terrestrial airborne SARs is to send out a pulse and receive the expected echoes before sending out the subsequent pulse. This places constraints on range vs. velocity parameters for the SAR, otherwise significantly complicating the radar design and operation.

We continue with the presumption that the effective pulse width of the SAR is equal to the actual transmitted pulse width. For matched-filter pulse compression this is the case, and for 'stretch' processing (deramping followed by a frequency transform) this is nearly the case and more so for small scene extents compared with the pulse width.

By insisting that the echo return before the subsequent pulse is emitted, we insist that

$$\left(T_{eff} + \frac{2}{c}R\right) \le \frac{1}{f_p} \tag{57}$$

which can be manipulated to

$$R \le \frac{c(1-d)}{2f_p} \tag{58}$$

and furthermore to

$$R \le \frac{c(1-d)D_{az}}{4k_a v_x} \tag{59}$$

The maximum R that satisfies this expression is often referred to as the 'unambiguous range' of the SAR. We note that the unambiguous range decreases with increasing velocity, increasing duty factor, and increasing k_a. The unambiguous range increases with a larger real antenna aperture azimuth dimension, due to a lower required PRF. Furthermore, the unambiguous range is frequency independent (for constant real apertures).

Figure 7 plots unambiguous range vs. velocity for several duty factors and antenna dimensions.
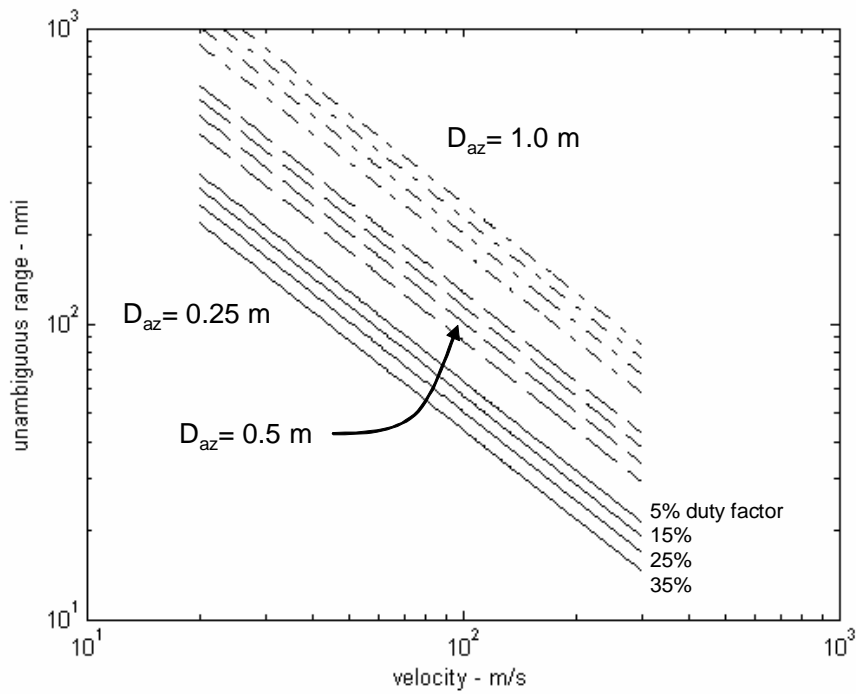
Figure 7. Unambiguous range limits for k_a=1.5.

If we need to work at a range beyond the unambiguous range, we need to either extend the unambiguous range (by appropriately modifying the radar antenna, duty factor, velocity, or oversampling factor k_a), or we need to operate with pulses 'in the air', that is, transmitting new pulses before the expected arrival of a previous pulse's echo. This is entirely possible and is in fact routine in space-based SAR (where often perhaps a dozen or more pulses are transmitted prior to receiving an echo from the first pulse).

Preferred Geometry for Pulses in the Air

The long ranges and high-velocities of orbital SAR systems often necessitate that the radar's PRF be selected in a manner to send out multiple pulses before the echo from the first pulse is received. That is, the pulse period is less than (sometimes substantially less than) the round-trip echo delay from the target scene. Consequently, echoes suffer a range ambiguity. Pulse coding can 'wash out' ambiguous range energy, but otherwise not eliminate it. Though antenna patterns can help attenuate ambiguous range returns, they cannot generally eliminate them entirely. If a surface reflector is strong enough to overcome the attenuation of the antenna beam, it will degrade the SAR image. One problematic bright reflector for orbital systems is the nadir point below the SAR. It is advantageous to select geometries and radar parameters such that any nadir echo does not coincide with legitimate target echoes.

The nadir echo will be at least as long in duration as the transmitted pulse, and in fact somewhat longer due to variations in the topography in the vicinity of nadir, as well as the curvature of the surface.

Long pulses are desired to maximize radar duty factor, and ultimately SNR in the SAR image. This exacerbates the nadir echo problem.

In pulse echo radar systems, the receiver is disengaged from data collection during the transmission of a pulse. Consequently, an ideal situation is then if the nadir return coincides with a transmitted pulse. This maximizes the time available to receive uncorrupted data, and in turn maximizes the pulse length that can be used. The penalty is that this places restrictions on the geometry that can be employed for SAR imaging.

Nevertheless, in systems where power is difficult to be had, and the mission parameters allow adjustments to imaging geometry, operating in one of the 'sweet spots' may offer considerable value, i.e., reduction in transmitter power required.

Consider the radar pulse train of Figure 8.
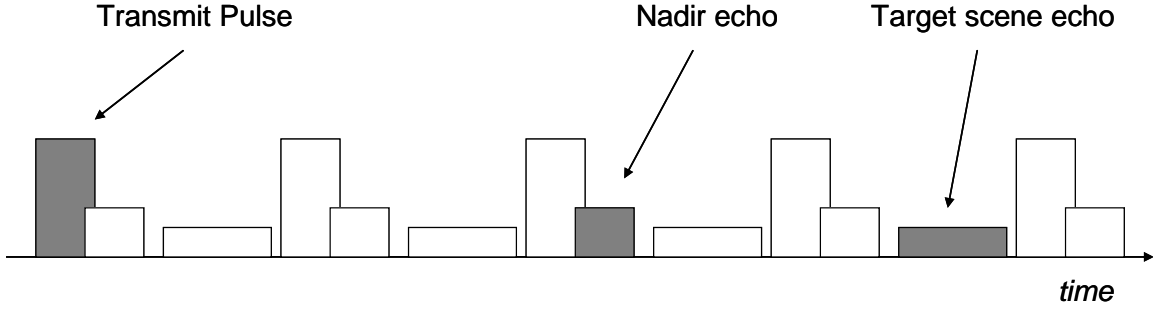
Figure 8. Radar pulse train with nadir and target scene echoes. The shaded transmit pulse corresponds to shaded nadir and target scene echoes.

We define

m_p = number of transmitted pulses 'in the air' between radar and target scene,
n_p = number of pulses 'in the air' between radar and nadir,
T_p = radar pulse period $= 1/f_p$, and
c = velocity of propagation. (60)

In Figure 8, $m_p=3$ and $n_p=2$. To cause the target scene echo to fall half-way between two transmitted pulses requires

$$\left(m_p + \frac{1}{2}\right)T_p = \frac{2}{c}R .$$ (61)

To cause the nadir return to fall on top of a transmitted pulse requires

$$n_p T_p = \frac{2}{c}h .$$ (62)

Consequently, for nadir to be occluded or eclipsed by a transmitted pulse requires the geometric constraint

$$\frac{h}{R} = \frac{n_p}{m_p + 1/2}$$ (63)

for integer values of m_p and n_p. Note that this requires

$$n_p \le m_p .$$ (64)

Typically for an orbital SAR, the radar height is dictated to the designer by other criteria. The task to the designer is then to select some optimized values of m_p and n_p, subject to the constraints above, which in turn defines a geometry and radar PRF.

Orbital SAR examples are given in Appendix C.

- 34 -

3.5 Extending Range

Extending the range of a SAR is equivalent to

1) ensuring that an adequate SNR is achievable at the new range of interest, and

2) ensuring that the unambiguous range constraint is adequately dealt with.

The unambiguous range issue was addressed in the last section. Here we address methods for increasing SNR at some range of interest.

We begin by recalling the expression for SNR in the SAR image, that is

$$SNR_{image} = \frac{P_{avg}\left(\eta_{ap}^2 A_A^2\right)\rho_r \sigma_{0,ref}\left(\dfrac{f}{f_{ref}}\right)^n f\, a_{wa}}{(8\pi)cv_x\left(kTF_N\right)\left(L_{radar}L_r L_a\right)\left(R^3\sqrt{1-\left(\dfrac{h}{R}\right)^2}\, 10^{\frac{\alpha R}{10}}\right)}. \tag{65}$$

A discussion of increasing SNR needs to examine what we can do with the individual parameters within the equation.

3.5.1 Increasing Average TX Power

We recall that the average TX power is the product of the peak TX power and the duty factor of the radar. Obviously we can increase the average power by increasing either one of these constituents, as long as it is not at the expense of the other. For example, a 100-W power amplifier operating at 30% duty factor is still better than a 200-W power amplifier operating at only a 10% duty factor, as far as SNR is concerned.

For a given TX power amplifier operating at full power, all we can do is ensure that we are operating at or near its duty factor limit. Since

$$P_{avg} = P_t d = P_t T_{eff} f_p \tag{66}$$

this is accomplished by increasing either or both the pulse width T_{eff} and the radar PRF f_p. If the radar PRF is constrained by an unambiguous range requirement, then the pulse width must be extended. For fine resolution SARs employing stretch processing we identify

$$T_{eff} = \frac{I}{f_s} \tag{67}$$

where

I = the total number of (fast-time) samples collected from a single pulse, and
f_s = the ADC sampling frequency employed.

We note that to satisfy Nyquist criteria using quadrature sampling,

$$f_s \geq B_{IF} \tag{68}$$

where B_{IF} is the IF bandwidth of the SAR.

Consequently, increasing the pulse width requires either collecting more samples I, or decreasing the ADC sampling frequency f_s (and the corresponding IF filter bandwidth B_{IF}).

Two important issues need to be kept in mind, however. The first is that extending the pulse width restricts the nearest range that the radar can image. That is, the TX pulse has to end before the near range echo arrives. The second is that the number of samples I restricts the range swath of the SAR image to $(B_{IF}/f_s)I$ resolution cells. The consequence to this is that relatively wide swaths at near ranges requires lots of samples I at very fast ADC sampling rates with corresponding wide IF filter bandwidths.

At far ranges, where near-range timing is not an issue, for a fixed IF filter bandwidth and ADC sampling frequency, we can always increase pulse width by collecting more samples I. If operating near the unambiguous range, however, prudence dictates that we remain aware that increasing the duty factor does in fact reduce the unambiguous range somewhat.

Operating beyond the unambiguous range limit requires a careful analysis of the radar timing in order to maximize the duty factor, juggling a number of additional constraints. It's enough to make your head spin.

Stretch processing derives no benefit from a duty factor greater than about 50%. A reasonable limit on usable duty factor due to other timing issues is often in the neighborhood of about 35%.

In any case, the easiest retrofit to existing SARs for increasing average TX power (and hence range) are first to increase the PRF to the maximum allowed by the timing, and second to increase the pulse width, with a corresponding increase in number of samples collected.

Furthermore, we note that at times it may be advantageous to shorten the pulse and increase the PRF, even if it means operating with pulses in the air (beyond the reduced unambiguous range), just to increase the duty factor. This is particularly true when the hardware is limited in how long a pulse can be transmitted.

3.5.2 Increasing Antenna Area

A bigger antenna (in either dimension) and/or better efficiency will yield improved SNR.

The down side is that a bigger azimuth dimension to the antenna aperture will restrict continuous strip mapping to coarser resolutions by the well known equation

$$\rho_a \geq \frac{D_{az}}{2} \qquad \text{(for strip mapping).} \tag{69}$$

Furthermore a bigger elevation dimension for the antenna aperture will reduce the illuminated range swath, thereby restricting perhaps the imaged range swath, especially at steeper depression angles. An additional subtle point is that as the elevation beamwidth narrows and gain improves, there comes a point when even as the SNR at the center of the beam still increases, nevertheless the SNR near the beam edge in fact decreases due to roll-off.

However, we note that in the SNR equation, antenna area and efficiency are squared. Consequently, doubling either one of these is equivalent to four times an increase in average TX power.

3.5.3 Selecting Optimal Frequency

As previously discussed, there is a clear preference for operating frequency depending on range, altitude, and weather conditions. For example, at a 50-nmi range from a 25-kft AGL altitude with 4 mm/Hr rain, X-band offers a 12.9 dB advantage over Ku-band. For perspective, a 1-kW Ku-band amplifier would provide performance equivalent to a 51-W X-band amplifier (for the same real antenna aperture, efficiency, yadda, yadda, yadda....).

Choice of operating frequency does need to be tempered, however, by the factors noted earlier in this report.

Interestingly, there may even be significant differences within the same radar band. For example, at 25 kft AGL altitude, within the international Ku-band (15.7 GHz to 17.7 GHz) the bottom edge provides 1.25 dB better SNR than the top edge at 20 nmi, 2.4 dB better SNR at 30 nmi, 3.5 dB better performance at 40 nmi, and 4.7 dB better performance at 50 nmi. Clearly, it seems advantageous to operate as near to the optimum frequency as the hardware and frequency authorization allow.

3.5.4 Modifying Operating Geometry

Once above the water-cloud layer, increasing the radar altitude will generally yield reduced average atmospheric attenuation, and hence improved transmission properties for a given range. Consequently, SNR is improved with operation at higher altitudes for any particular typical weather condition.

This translates to increased range at higher altitudes.

3.5.5 Coarser Resolutions

SNR is directly proportional to slant-range resolution. However in the radar equation as presented, no overt effect is obvious due to changing azimuth resolution. This is because as azimuth resolution gets finer, the target cell RCS diminishes as expected, but also the synthetic aperture lengthens correspondingly thereby increasing coherent processing gain and exactly countering the effects of diminished RCS. The net effect is no change to SNR.

Consequently, only range resolution influences SNR.

The next several figures illustrate how range-performance in both clear air and adverse weather depends on operating geometry and resolution. Acceptable SNR performance is achievable to the left of the curves corresponding to a particular resolution.

We note that 1 nmi (nautical mile) = 1.852 kilometers, and 1 kft = 304.8 meters. Furthermore, 1 kt = 0.514444 m/s approximately.

Frequency = 16.7 GHz	Velocity (ground speed) = 70 kts
Power (peak) = 320 W	Noise reflectivity = -25 dB
duty factor = 0.35	Losses (signal processing) = 2 dB
Antenna (ap area) = 93.0002 sq in	Losses (radar) = 2 dB
Antenna (ap aspect) = 2.7	Noise figure = 4 dB
Antenna (gain) = 30.6812 dB	Unambiguous range = 196 nmi
Antenna (ap pwr dens) = 3.44 W/si	(resolution in "m")
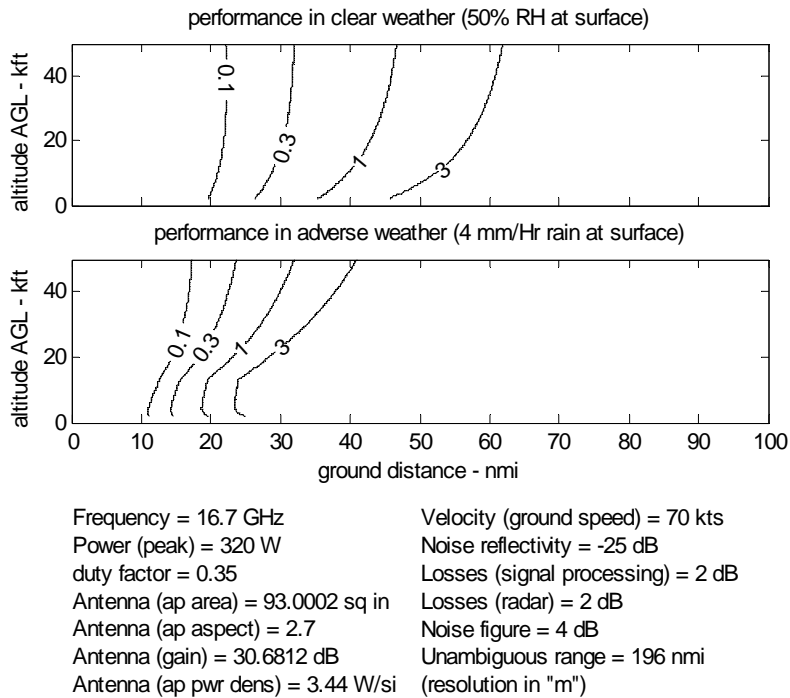
Figure 9. Geometry limits vs. resolution.

performance in clear weather (50% RH at surface)

performance in adverse weather (4 mm/Hr rain at surface)

Frequency = 16.7 GHz	Velocity (ground speed) = 250 kts
Power (peak) = 700 W	Noise reflectivity = -25 dB
duty factor = 0.35	Losses (signal processing) = 2 dB
Antenna (ap area) = 297 sq in	Losses (radar) = 2.7 dB
Antenna (ap aspect) = 1.6296	Noise figure = 3.2 dB
Antenna (gain) = 35.0689 dB	Unambiguous range = 76 nmi
Antenna (ap pwr dens) = 2.36 W/si	(resolution in "m")

Figure 10. Geometry limits vs. resolution.

performance in clear weather (50% RH at surface)

performance in adverse weather (4 mm/Hr rain at surface)

Frequency = 16.7 GHz	Velocity (ground speed) = 70 kts
Power (peak) = 80 W	Noise reflectivity = -25 dB
duty factor = 0.35	Losses (signal processing) = 2 dB
Antenna (ap area) = 60.5 sq in	Losses (radar) = 2 dB
Antenna (ap aspect) = 2	Noise figure = 4 dB
Antenna (gain) = 28.5452 dB	Unambiguous range = 136 nmi
Antenna (ap pwr dens) = 1.32 W/si	(resolution in "m")

Figure 11. Geometry limits vs. resolution.

performance in clear weather (50% RH at surface)

performance in adverse weather (4 mm/Hr rain at surface)

Frequency = 9.6 GHz	Velocity (ground speed) = 70 kts
Power (peak) = 80 W	Noise reflectivity = -25 dB
duty factor = 0.35	Losses (signal processing) = 2 dB
Antenna (ap area) = 60.5 sq in	Losses (radar) = 2 dB
Antenna (ap aspect) = 2	Noise figure = 4 dB
Antenna (gain) = 23.7363 dB	Unambiguous range = 136 nmi
Antenna (ap pwr dens) = 1.32 W/si	(resolution in "m")

Figure 12. Geometry limits vs. resolution.

performance in clear weather (50% RH at surface)

performance in adverse weather (4 mm/Hr rain at surface)

Frequency = 35 GHz	Velocity (ground speed) = 70 kts
Power (peak) = 80 W	Noise reflectivity = -25 dB
duty factor = 0.35	Losses (signal processing) = 2 dB
Antenna (ap area) = 60.5 sq in	Losses (radar) = 2 dB
Antenna (ap aspect) = 2	Noise figure = 4 dB
Antenna (gain) = 34.9723 dB	Unambiguous range = 136 nmi
Antenna (ap pwr dens) = 1.32 W/si	(resolution in "m")

Figure 13. Geometry limits vs. resolution.

3.5.6 Decreasing Velocity

SNR is really a function of the total energy collected from the target scene. Total energy, of course, is the average power integrated over the aperture time. Consequently, a longer aperture time yields a better SNR. We achieve a longer aperture time for a fixed aperture length by flying slower, that is, collecting data at a reduced velocity. Hence, collecting data at a slower velocity allows a greater SNR in the image, due to a greater coherent integration gain.

However, what is important is not the actual velocity of the aircraft, but rather the translational velocity v_x defined to be the horizontal velocity orthogonal to the direction to the target scene. If the aircraft is traveling in a direction not horizontal and orthogonal to the direction towards the target scene, then the important parameter v_x is that component of the aircraft velocity that is. This brings in the notion of 'squint' angle, illustrated in figure 14.
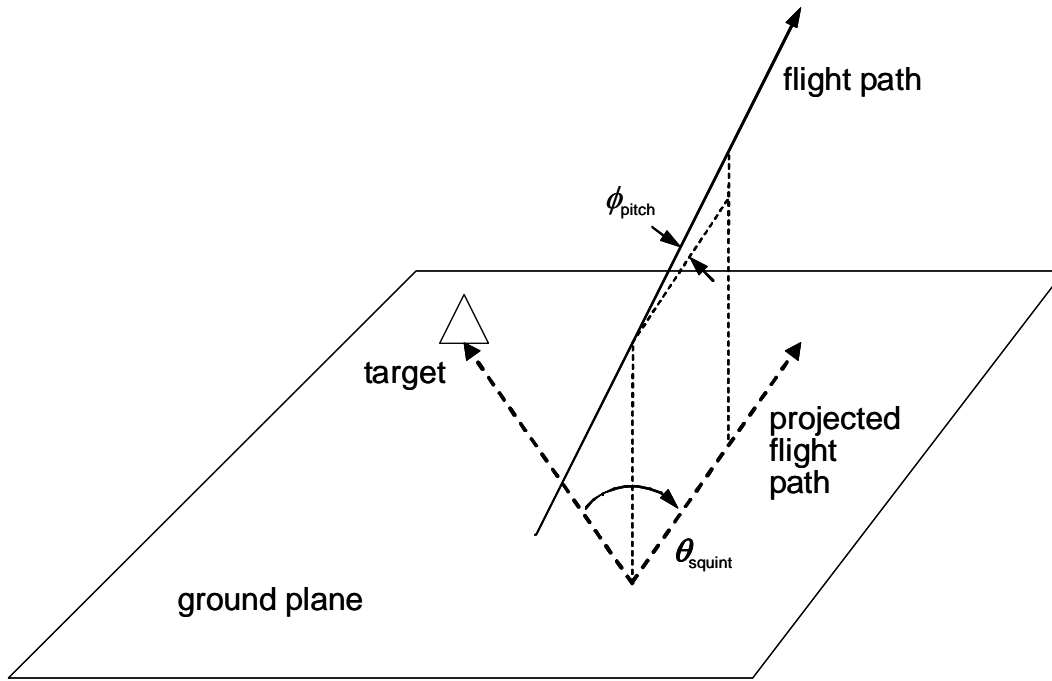
Figure 14. Flight path geometry definitions.

The aircraft might be flying with a velocity $v_{aircraft}$, but with a squint angle θ_{squint} and pitch angle ϕ_{pitch} with respect to the target. The velocity component of interest, that is, the velocity component that influences SNR is

$$v_x = v_{aircraft} \cos\phi_{pitch} \sin\theta_{squint} \tag{70}$$

where

$v_{aircraft}$ = the magnitude of the aircraft velocity vector,

ϕ_{pitch} = the pitch angle of the velocity vector, and

θ_{squint} = the squint angle to the target (as projected on the ground). (71)

Nominally, SAR collects data from a level flight path ($\phi_{pitch} = 0$), and a broadside geometry ($\theta_{squint} = 90^{\,o}$). Clearly, one way to reduce the velocity component v_x is to squint forward sufficiently. For example, at $\theta_{squint} = 45^{\,o}$, we calculate $v_x = 0.707\, v_{aircraft}$, with a corresponding potential increase in SNR of 1.5 dB.

This improves much more for more severe squint angles. The down side to more severe squint angles are more severe geometric distortions in the SAR image, and an increase in required bandwidth.[9]

It is also important to note that unambiguous range is extended with a reduced v_x.

Another way to effectively increase the total aperture time (and hence SNR) is to coherently combine data from multiple collection passes. Noncoherent integration of distinct SAR images can also offer improvement in some cases.

3.5.7 Decreasing Radar Losses, Signal Processing Losses, and System Noise Factor

Any reduction in system losses yields a SNR gain of equal amount. This is also true of reducing the system noise factor. For example, reducing the TX amplifier to antenna loss by 1 dB translates to a 1-dB improvement in SNR. Likewise, a 2-dB reduction in system noise factor translates to a 2-dB improvement in SNR.

We note that high-power devices such as duplexers, switches, and protection devices tend to be lossier than lower power devices. Consequently, doubling the TX power amplifier output power might require lossier components elsewhere in the radar, rendering less than a doubling of SNR in the image. Furthermore, high-power microwave switches tend to be bulkier than their low-power counterparts, requiring perhaps longer switching times which may impact achievable duty factors.

3.5.8 Easing Weather Requirements

Atmospheric losses are less in fair weather than in inclement weather. Consequently SNR is improved (and range increased) for a nicer atmosphere. In real life you get what you get in weather, although a data collection might make use of weather inhomogeneities (like choosing a flight path or time to avoid the worst conditions).

Weather attenuation models are very squishy (of limited accuracy) and prone to widely varying interpretations. Consequently, SAR performance claims might use this to advantage (and probably often do). The point of this is that while requests for proposals often contain a weather specification/requirement (e.g. 4 mm/Hr rain over a 10 nmi

swath), there is no uniform interpretation on what this means insofar as attenuation to radar signals.

3.5.9 Changing Reference Reflectivity

This is equivalent to the age-old technique of "If we can't meet the spec, then reduce the spec." We note that a radar that meets the common requirement of a 0-dB SNR with $\sigma_{0,ref} = -25$ dB at some range, will meet a 0-dB SNR for $\sigma_{0,ref} = -20$ dB at some farther range. SNR performance tends to degrade gracefully with range, consequently a tolerance for poorer image quality will result in longer range operation. The equivalent reflectivity of the noise in the SAR image is denoted as σ_N. That is,

$$\sigma_N = \sigma_0 \big|_{SNR_{image}=0\ dB}. \tag{72}$$

The following figures illustrate how artificially degrading the SNR in the image (by effectively increasing σ_N) affects image quality for a Ku-band SAR image of the Capitol building in Washington, DC. Depending on what we might be looking for, even fairly noisy images can still be usable. For example, the Capitol dome is still identifiable even with $\sigma_N = -15$ dB.

Figure 15. Ku-band SAR image with $\sigma_N < -30$ dB.

Figure 16. Ku-band SAR image with simulated $\sigma_N = -25$ dB.

Figure 17. Ku-band SAR image with simulated σ_N = −20 dB.

Figure 18. Ku-band SAR image with simulated σ_N = −15 dB.

4 Conclusions

The aim of this report is to allow the reader to understand the nature of relevant physical parameters in how they influence SAR performance. The radar equation can be (and was) transmogrified to a form that shows these parameters explicitly. Maximizing performance of a SAR system is then an exercise in modifying the relevant parameters to some optimum combination. This was discussed in detail.

Nevertheless, some observations are worth repeating here.

For lots of power over wide bandwidths, active phased arrays look like the way to go. Current technology offers 10 W per square centimeter at X-band. Experimental MMICs are already demonstrating many tens of Watts at Ku-band.

Atmospheric losses are typically greater at higher frequency, in heavier rainfalls, and at lower altitudes. These conspire to indicate an optimum operating frequency for a constrained antenna area at any particular operating geometry and weather condition.

For a fixed antenna size, optimum PRF is independent of radar frequency.

The direct return from rain should not generally be a problem in a typical SAR image, unless we are flying really fast and imaging at the higher radar frequencies at relatively coarse resolutions in particularly heavy rain.

Imaging at long ranges from high velocities will necessitate pulses in the air. This is made worse by small antenna dimensions, and higher duty factors. When necessary, optimal geometries exist for this.

Extending the range of a SAR system can be done by incorporating any of the following:

> increasing average TX power (peak TX power and/or duty factor)
> increasing antenna area and/or efficiency
> operating in a more optimal radar band (or portion of a radar band)
> flying at a more optimal altitude (usually higher)
> operating with coarser range resolution (azimuth resolution doesn't help)
> decreasing tangential velocity (decreasing velocity, or more severe squint angles)
> decreasing system losses and/or system noise factor
> operating in more benign weather conditions
> degrading the noise equivalent reflectivity required of the scene

References

[1] Armin W. Doerry, "Performance Limits for Synthetic Aperture Radar", Sandia Report SAND2001-0044, January 2001.

[2] Fred E. Nathanson, *Radar Design Principles - second edition*, ISBN 0-07-046052-3, McGraw-Hill, Inc., 1991.

[3] A. W. Doerry, "Atmospheric loss considerations for synthetic aperture radar design and operation", SPIE 2004 Defense & Security Symposium, Radar Sensor Technology IX, Vol. 5410A, Orlando FL, 12-16 April 2004.

[4] A. Doerry, "Atmospheric attenuation and SAR operating frequency selection", Workshop on Synthetic Aperture Radar Technology", Redstone Arsenal, AL, October 22 & 23, 2003.

[5] F. M. Dickey, L. A. Romero, J. M. DeLaurentis, A. W. Doerry, "Superresolution, Degrees of Freedom and Synthetic Aperture Radar", IEE Proc.-Radar Sonar Navig., Vol. 150, No. 6, pp 419-429, December 2003.

[6] Merrill I. Skolnik, *Introduction to Radar Systems - second edition*, ISBN 0-07-057090-1, McGraw-Hill, Inc., 1980.

[7] Fred E. Nathanson, *Radar Design Principles - second edition*, ISBN 0-07-046052-3, McGraw-Hill, Inc., 1991.

[8] Richard J. Doviak, Dusan S. Zrnic, *Doppler Radar and Weather Observations - second edition*, ISBN 0-12-221422-6, Academic Press, Inc., 1993.

[9] Doerry, Armin, "Bandwidth requirements for fine resolution squinted SAR", SPIE 2000 International Symposium on Aerospace/Defense Sensing, Simulation, and Controls, Radar Sensor Technology V, Vol. 4033, Orlando FL, 27 April 2000.

Matlab files used:

atmrate2
snrvsf.m
optimalf.m
raincltr.m
snrvsgeo.m
resvsgeo.m
unamb_rng.m

This page left intentionally blank.

Appendix A – Processing Gain Details

Introduction & Background

Synthetic Aperture Radar (SAR) systems by definition perform coherent processing of echoes from multiple pulses. This allows for improved azimuth resolution as well as Signal to Noise Ratio (SNR) enhancement, otherwise known as azimuth processing gain. SAR systems also routinely use modulation schemes to enhance the bandwidth of their signals in order to better range resolution, also providing range processing gain. Herein we explore issues of determining what the processing gains really are, even in the presence of sidelobe reduction techniques such as employing window functions.

Radar Range Equation Preliminaries

Recall that by including processing gains due to pulse compression and coherent pulse integration, the net SNR in the image becomes

$$SNR_{image} = \frac{P_t G_A{}^2 \lambda^2 \sigma_0 \rho_a \rho_r}{(4\pi)^3 R^4 \cos\psi_g (kTF_N) B_N L_{radar} L_{atmos}} G_r G_a \qquad \text{(A-1)}$$

where

G_r = range processing gain (due to pulse compression),

G_a = azimuth processing gain (due to multiple coherent pulse integration), and

other parameters remain as defined in the body of this report. (A-2)

SAR processing is essentially matched filtering the cumulative data set to the expected returns from a pixel of interest, and is done for each pixel in an image. Transform techniques are employed for efficiency of processing. Range and azimuth processing are, to first order, separable. Consequently the total matched filter can be separated into range processing and azimuth processing, that is, the combination of separate matched filtering in range and matched filtering in azimuth. The separate gain parameters in the *SNR* equation above presume this. We shall consider them individually below.

Matched Filter Basics

Derivation of matched filter characteristics and properties are straightforward, and discussed in many texts.[1,2,3] The Matched Filter derives its name from the fact that it is optimized (matched) for an expected input signal.

Assume an input signal $x(t)$ corrupted with additive White Gaussian Noise (WGN) $n(t)$ with Power Spectral Density (PSD) of $N_0/2$. This is input to a Matched Filter (matched to $x(t)$). The signal component of the Matched filter output is

$$y_{MF}(t) = \int_{-\infty}^{\infty} x(\tau)x*(\tau - t)d\tau \qquad \text{(A-3)}$$

where * denotes complex conjugate. This is identified as the autocorrelation function of $x(t)$. At its output peak, the Matched Filter is optimum in maximizing the SNR, and is given by

$$SNR_{MF,output} = \frac{2E}{N_0} \qquad \text{(A-4)}$$

where E is the energy in the signal $x(t)$.

Consider that the input signal $x(t)$ has effective duration of T_{eff}. Furthermore consider that the noise $n(t)$ has finite bandwidth B_N, which we shall assume is also greater than the finite bandwidth of $x(t)$. Note that we cannot have both a finite bandwidth and finite duration signal in absolute terms, but we can nevertheless have signals for which an overwhelming fraction of their energy is contained within some finite bandwidth, and within some time duration, such that effective limits are reasonable. Consequently, the input to the Matched filter has SNR

$$SNR_{MF,input} = \frac{\left(\dfrac{E}{T_{eff}}\right)}{\left(\dfrac{N_0}{2}B_N\right)} = \frac{2E}{N_0}\left(\frac{1}{T_{eff}B_N}\right). \qquad \text{(A-5)}$$

Consequently, at the location of the autocorrelation peak, the output SNR will have improved the SNR by the time-bandwidth product of the signal. That is, the matched filter SNR gain is

$$G_{MF} = \frac{SNR_{MF,input}}{SNR_{MF,output}} = T_{eff}B_N. \qquad \text{(A-6)}$$

It is critical to understand that the output SNR for a Matched Filter is dependent solely on the signal energy, and the PSD of the noise, regardless of any input signal or input noise bandwidth. However, input SNR does depend on noise bandwidth, as well as average signal power. Consequently, seemingly paradoxically, SNR gain can always be improved by letting more noise bandwidth into the Matched Filter, thereby decreasing input SNR, but output SNR nevertheless remains unaffected. This is because the Matched Filter is already, after all, an optimal noise reduction filter.

Rectangular Power Spectral Density Signals

A particularly interesting class of signals to radar systems exhibits a power spectral density shaped as a $rect(.)$ function, that is

$$PSD(f) = rect\left(\frac{f - f_0}{B_T}\right) \tag{A-7}$$

where f_0 is some nominal center frequency, B_T is the signal bandwidth, and

$$rect(f) = \begin{cases} 1 & f < 1/2 \\ 0 & else \end{cases} \tag{A-8}$$

as illustrated in figure A-1. This is for all practical purposes the case, for example, for Linear FM chirps with high time-bandwidth products.
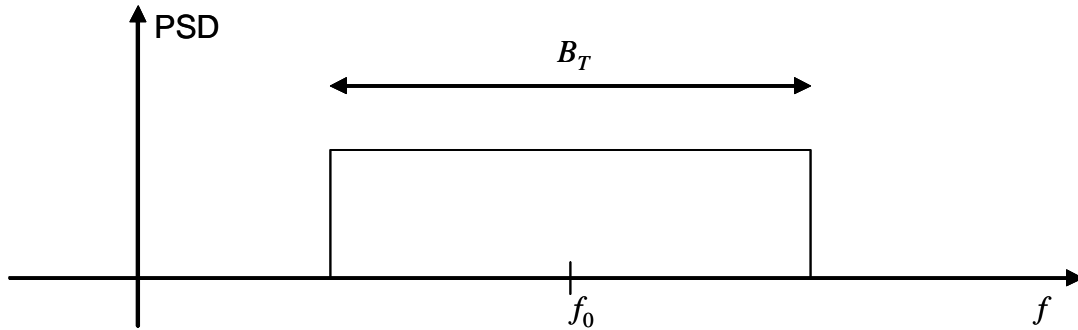
Figure A-1. Signal Power Spectral Density.

The Fourier Transform of the PSD yields the autocorrelation function. Consequently, the matched filter output of a signal with PSD given in figure 1 has characteristics

$$|y_{MF}(t)| = B_T \text{sinc}(B_T t) \tag{A-9}$$

where $\text{sinc}(t) = \dfrac{\sin \pi t}{\pi t}$.

For signals with 'not exactly' this PSD, or for signals with effectively finite duration T_{eff}, the sinc function nature of the matched filter output is still typically a very good approximation in the region of maximum response, i.e. the main lobe of the sinc function.

A representative output of the matched filter response centered at time t_0 is given in figure A-2.
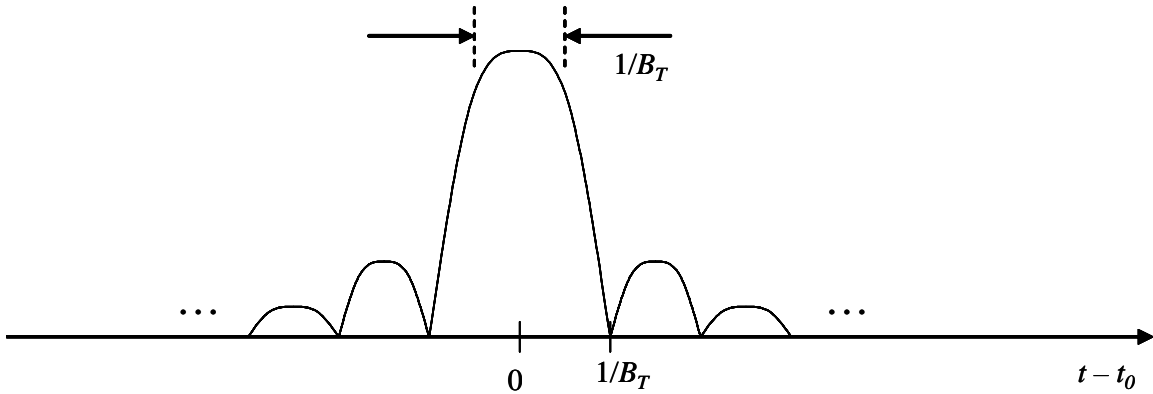
Figure A-2. Matched Filter output.

Note that most of the energy is located within an interval of width $1/B_T$, but that significant energy still exists in sidelobes that extend considerably from the mainlobe.

Nevertheless, a signal with original effective duration T_{eff} at the input to the matched filter has been 'compressed' to a new signal at the output of the matched filter with width $1/B_T$. Consequently the signal has a compression ratio of

$$compression\_ratio = \frac{T_{eff}}{1/B_T} = T_{eff} B_T \qquad \text{(A-10)}$$

which is coincidentally the same as the SNR gain for $B_N = B_T$. This is sometimes referred to as the 'compression gain'.

Note, however, that the width of the matched filter output, though stipulated to be $1/B_T$, is somewhat arbitrary. For example, the null-to-null width is $2/B_T$, and the −3 dB width is approximately $0.88/B_T$. Selecting a new measure for 'width' will impact the compression ratio, but not the SNR gain.

If we define a relative width factor a_w such that the matched filter output has width designated to be a_w/B_T , as in figure A-3,
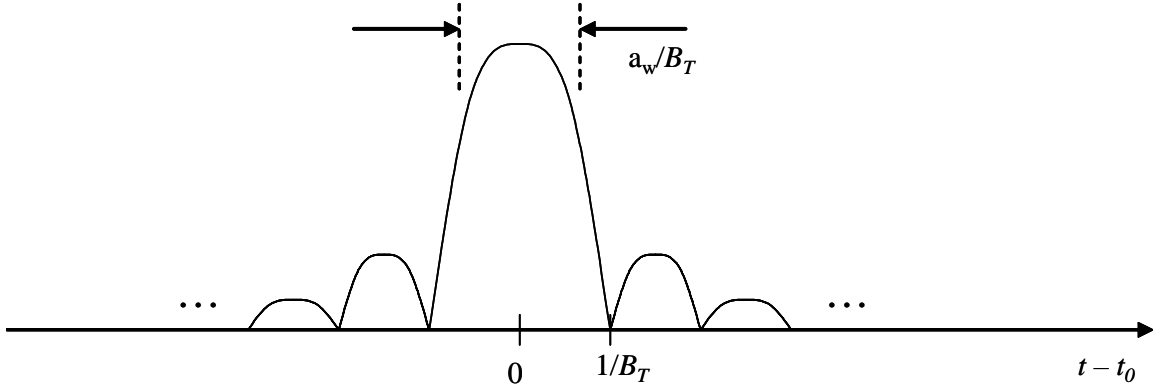
Figure A-3. Matched Filter output.

then the compression ratio becomes

$$compression\_ratio = \frac{T_{eff} B_T}{a_w} \tag{A-11}$$

but the SNR gain remains $T_{eff} B_N$. This subtlety is sometimes a point of confusion, and leads to erroneously interchanging compression ratio with SNR gain.

Sidelobe Reduction by Filtering with Window Functions

The sidelobes at the output of a matched filter are problematic, and their mitigation is sought often at the expense of sub-optimal performance in both the compression ratio and SNR gain.

Sidelobe mitigation is most commonly accomplished with additional linear low-pass filtering. Typically, this additional linear low-pass filtering is implemented with the application of a window function to the Fourier transform of the Matched Filter output. That is, since Matched Filtering is often implemented using fast correlation/convolution with Fourier Transforms, the window is applied prior to the final transform that yields the final output. Nevertheless, it is still a linear filtering operation.

Since Matched Filtering without sidelobe mitigation is optimal with respect to output SNR, any additional filtering renders the final output suboptimal with respect to SNR. Consequently SNR gain due to processing becomes

$$G_{processing} = \frac{T_{eff} B_N}{L_{processing}} \tag{A-12}$$

where $L_{processing}$ is a loss with respect to a Matched Filter without any additional sidelobe mitigation filtering. For many commonly used window functions, $L_{processing}$ is on the order of 1 dB.

The additional sidelobe filtering also unavoidably 'blurs' the Matched Filter output, widening its mainlobe. But since mainlobe width is already a somewhat arbitrary measure, we can continue with the definition of a relative width factor a_w such that the matched filter output has width designated to be a_w/B_T, as in figure A-4,
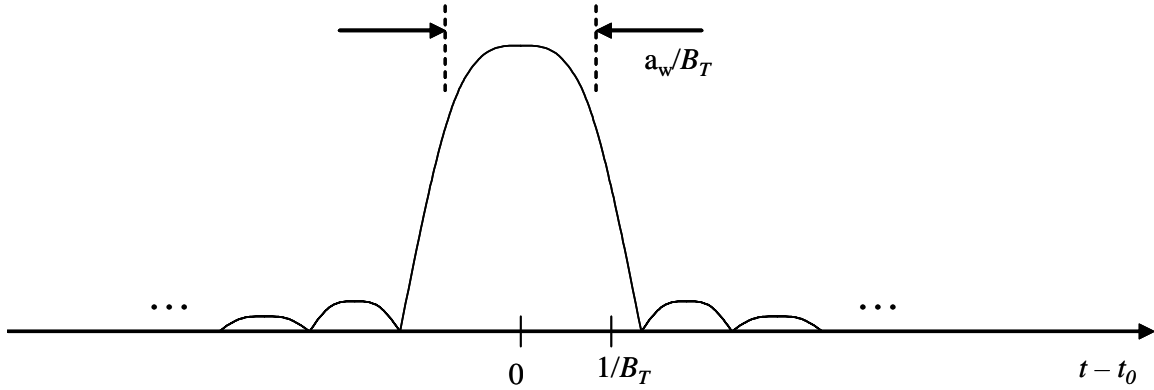
Figure A-4. Matched Filter output after sidelobe filtering.

with the compression ratio remaining

$$compression\_ratio = \frac{T_{eff} B_T}{a_w} \, . \tag{A-13}$$

A common measure for the matched filter output width, or resolution, is the -3 dB width. Consequently, a_w is then presumed to be the ratio of the actual -3 dB width to the nominal width $1/B_T$. Often, satisfactory sidelobe mitigation can be had with window functions that exhibit a_w in the range of 1.1 to 1.5 or so.

It remains important to note, however, that processing gain and compression ratio, while close, nevertheless are different numbers. That is, they are different whenever $a_w \neq L_{processing}$. This is an often overlooked subtlety.

Table A-1 compares some parameters of popular windows. Interestingly, while $a_w \neq L_{processing}$ exactly, for many window functions they do tend to be close, often within a fraction of a dB.

Table A-1. Popular window function parameters.

Window Function Name	a_w (at -3 dB point)	$L_{processing}$	Peak Sidelobe Level (dBc)
Rectangular (Boxcar)	0.88	1.0 (0.0 dB)	-13.3
Hamming	1.30	1.37 (1.36 dB)	-42.7
Hanning	1.43	1.49 (1.74 dB)	-31.5
Blackman	1.65	1.73 (2.39 dB)	-58.1
Taylor (35 dB, $\bar{n} = 4$)	1.18	1.23 (0.91 dB)	-35.2
Taylor (40 dB, $\bar{n} = 6$)	1.25	1.30 (1.15 dB)	-40.2
Triangle	1.27	1.33 (1.25 dB)	-26.5

Range Processing Gain

Range processing for SAR is essentially Match Filtering (or correlation) of the radar echoes. In practice, a variety of waveforms are used including Linear FM chirps, phase-coded pulses, pseudo-noise, extremely short pulses, continuous FM, and others. However, regardless of what waveform is used, each still exhibits some finite bandwidth B_T, and exhibits some effective duration T_{eff}, in the echo data.

Furthermore, after Matched Filtering and any additional filtering for sidelobe control, the output signal will still exhibit SOME amount of SNR gain. This range processing gain can still be written as

$$G_r = \frac{T_{eff} B_N}{L_r} \tag{A-14}$$

where L_r is range processing loss with respect to an ideal gain of $T_{eff} B_N$.

Furthermore still, whatever waveform is used will have a PSD that corresponds to SOME autocorrelation function, that with any additional filtering has SOME mainlobe width. Consequently, the range processing output will still have a timing resolution of a_{wr}/B_T, where a_{wr} is the actual mainlobe width with respect to $1/B_T$. This results in a range processing compression ratio that can still be written as

$$compression\_ratio = \frac{T_{eff} B_T}{a_w} . \tag{A-15}$$

SAR range resolution relates to timing resolution by

$$\rho_r = \left(\frac{c}{2}\right)\frac{a_{wr}}{B_T} \tag{A-16}$$

where c is velocity of propagation. Rearranging this yields a signal bandwidth requirement to achieve a particular resolution as the familiar

$$B_T = a_{wr}\left(\frac{c}{2\rho_r}\right).$$ (A-17)

We emphasize that these equations are fairly general and apply to a wide variety of waveforms.

Azimuth Processing Gain

Azimuth processing for SAR is essentially coherently combining the echoes from multiple pulses that form the synthetic aperture. This is also a Matched Filtering operation. Gain and compression characteristics may be computed from a number of different perspectives.

Fundamentally, if N equally spaced pulses along a synthetic aperture are coherently processed with equal weighting in the Matched Filter, then the SNR gain due to azimuth processing is N, as is the nominal compression ratio. By applying sidelobe control filtering, i.e. using window functions, then

$$G_a = \frac{N}{L_a}$$ (A-18)

where L_a is azimuth processing loss with respect to an ideal SNR gain of N. With respect to azimuth processing, we identify

$$N = T_{ap} f_p$$ (A-19)

where

f_p = the radar pulse repetition frequency, and

T_{ap} = the synthetic aperture flight/collection time. (A-20)

Note that $T_{ap} f_p$ is in fact a time-bandwidth product where f_p is a noise bandwidth resulting from uncorrelated pulse-to-pulse noise.

We also note that

$$T_{ap} = \frac{L_{ap}}{v_x}$$ (A-21)

where, assuming broadside imaging,

L_{ap} = the synthetic aperture length, and

v_x = the velocity with which the synthetic aperture is flown. (A-22)

At imaging geometries other than broadside, these are replaced with their tangential component values.

The purpose of a synthetic aperture is to allow azimuthal resolution to something finer than the azimuth beamwidth of the real antenna. With SAR, azimuthal angle corresponds to Doppler frequency. The Doppler bandwidth of a scene due to the real antenna is nominally

$$B_{Doppler} = \frac{2}{\lambda} v_x \theta_{az}$$ (A-23)

where θ_{az} is the beamwidth of the real antenna. We typically operate such that $f_p > B_{Doppler}$. The output of the combined Matched Filter and sidelobe mitigation resolves Doppler to a resolution of

$$\rho_{Doppler} = a_{wa} \frac{1}{T_{ap}} = a_{wa} \frac{f_p}{N}$$ (A-24)

where a_{wa} is the mainlobe width with respect to f_p/N.

Since every pulse is also presumed to contain signal samples, the quantity f_p also represents the data bandwidth. Consequently, the compression ratio is then simply

$$compression\_ratio = \frac{f_p}{\rho_{Doppler}} = \frac{N}{a_{wa}}.$$ (A-25)

Actual azimuth spatial resolution is related to Doppler resolution by

$$\rho_a = \frac{\lambda R}{2v_x} \rho_{Doppler}$$ (A-26)

Combining some equations yields the familiar formula

$$\rho_a = a_{wa} \frac{\lambda R}{2L_{ap}}.$$ (A-27)

Finally, by taking advantage of some of these relationships, we expand the azimuth processing gain as

$$G_a = \frac{a_{wa}\left(\dfrac{f_p \lambda R}{2\rho_a v_x}\right)}{L_a}.$$
(A-28)

<u>*Summary*</u>

We emphasize the following points:

- Radar signal processing is essentially implementing a Matched Filter with perhaps some additional filtering typically for sidelobe control.

- Window functions prior to a Fourier Transform essentially implements a low-pass linear filter.

- Resolution enhancement is due to signal compression, and is limited to the width of the autocorrelation function of the radar signals employed, and the synthetic aperture collected. Filtering for sidelobe control can only broaden the autocorrelation mainlobe, and hence resolution.

- Processing gain is SNR enhancement, and is maximum for a Matched Filter. Any filtering for sidelobe control diminishes this gain somewhat. This gain diminishment is often referred to as a signal processing loss.

- Mainlobe broadening due to filtering for sidelobe control is not precisely equal to the signal processing loss, but is often close.

References

[1] Robert N. McDonough, Anthony D. Whalen, *Detection of Signals in Noise – Second Edition*, ISBN 0-12-744852-7, Academic Press, 1995.

[2] Wilbur B. Davenport, Jr., William L. Root, *An Introduction to the Theory of Random Signals and Noise*, ISBN 0-87942-235-1, IEEE Press, 1987.

[3] A. Bruce Carlson, Paul B. Crilly, Janet C. Rutledge, *Communication Systems – An Introduction to Signals and Noise in Electrical Communication – Fourth Edition*, ISBN 0-07-011127-8, McGraw-Hill, 2002.

Appendix B – Comparison to Literature

The image SNR equation was shown to be

$$SNR_{image} = \frac{P_{avg}G_A{}^2\lambda^3\sigma_0\rho_r a_{wa}}{2(4\pi)^3 R^3 v_x \cos\psi_g \left(kTF_N\right)L_{radar}L_{atmos}L_r L_a} .$$ (B-1)

When this is rewritten as,

$$SNR_{image} = \left[\frac{P_{avg}G_A{}^2\lambda^3\sigma_0\rho_y}{2(4\pi R)^3 v_x\left(F_N kT\right)}\right]a_{wa}\left(\frac{1}{L_{radar}L_{atmos}L_r L_a}\right)$$ (B-2)

where

$$\rho_y = \frac{\rho_r}{\cos\psi_g} = \text{ground-range resolution (as opposed to slant-range resolution), the term}$$

in the square brackets is equivalent to eq. 2.8.8 in Curlander & McDonough.[1] Sidelobe control and system losses are not addressed in this equation.

When the image SNR equation is rewritten as,

$$SNR_{image} = \left[\frac{P_{avg}A_e{}^2\sigma_0\rho_r\sec\psi_g}{2(4\pi)\lambda\left(kTF_N\right)v_x R^3}\right]a_{wa}\left(\frac{1}{L_{radar}L_{atmos}L_r L_a}\right)$$ (B-3)

where $A_e = \dfrac{G_A\lambda^2}{4\pi}$ = antenna effective area, the square brackets are now equivalent to eq. 14.15 in Skolnik.[2] Skolnik also neglects aperture tapering for sidelobe control, as well as various system losses. Skolnik also points out that his equation is consistent with Harger.[3]

When the image SNR equation is rewritten as,

$$SNR_{image} = \left[\frac{P_{avg}G_A{}^2\lambda^3\sigma_0}{(4\pi)^3 R^3 k\left(F_N T\right)\left(L_{radar}L_{atmos}\right)}\frac{\rho_r}{2v_x}\csc\left(\frac{\pi}{2}-\psi_g\right)\right]a_{wa}\left(\frac{1}{L_r L_a}\right)$$ (B-4)

the square brackets are equivalent to eq. 12.37 in Mahafza.[4] While system losses are included, sidelobe control is again omitted by this author.

When the image SNR equation is rewritten as

$$SNR_{image} = \left[\frac{P_{avg}G_A{}^2}{2(F_N kT)L_{radar}L_{atmos}}\left(\frac{\lambda}{4\pi R}\right)^3\left(\frac{\sigma_0\rho_r}{a_{wr}v_x\cos\psi_g}\right)\right]\frac{a_{wr}a_{wa}}{L_r L_a} \qquad \text{(B-5)}$$

where a_{wr} is the range broadening factor due to the range sidelobe mitigation filter, then the terms in the square brackets are equivalent to eq. 8.4 in Carrara, Goodman, & Majewski.[5] While system losses and sidelobe control are included in their equation, they tacitly make the presumption that $L_r = a_{wr}$ and $L_a = a_{wa}$ (which we showed earlier is often pretty close).

When the image SNR equation is rewritten as

$$SNR_{image} = \left[\frac{P_{avg}G_A{}^2\lambda^3 a_{wa}\sigma_0\rho_y}{2(4\pi)^3 R^3(kTF_N)v_x}\right]\left(\frac{1}{L_{radar}L_{atmos}L_r L_a}\right) \qquad \text{(B-6)}$$

the terms in the square bracket are almost, but not quite equivalent to eq. 9.64 in Ulaby, Moore, and Fung.[6] They develop the radar equation from the standpoint of an equivalent narrow pulse (no pulse compression, and hence no processing gain). However, their equation 9.63a contains a subtle but significant error, that when corrected equates receiver noise bandwidth with signal bandwidth to become (using our terms)

$$B_N = B_T = \frac{1}{T_{eff}} = \frac{a_{wr}c}{2\rho_r} \qquad \text{(B-7)}$$

Carrying this correction into their eq. 9.64 would cause it to be equivalent to the term in the square brackets above. Note that window broadening is accounted for by the authors, but losses are omitted.

References

[1] John C. Curlander, Robert N. McDonough, *Synthetic Aperture Radar, Systems & Signal Processing*, ISBN 0-471-85770-X, John Wiley & Sons, 1991.

[2] Merrill I. Skolnik, *Introduction to Radar Systems, second edition*, ISBN 0-07-057909-1, McGraw Hill, 1962.

[3] Robert O. Harger, *Synthetic Aperture Radar Systems, Theory and Design*, Academic Press, 1970.

[4] Bassem R. Mahafza, *Radar Systems Analysis and Design Using MATLAB*, ISBN 1-58488-182-8, Chapman & Hall / CRC, 2000.

[5] Walter G. Carrara, Ron S. Goodman, Ronald M. Majewski, *Spotlight Synthetic Aperture Radar, Signal Processing Algorithms,* ISBN 0-89006-728-7, Artech House, 1995.

[6] Fawwaz T. Ulaby, Richard K. Moore, Adrian K. Fung, *Microwave Remote Sensing, Active and Passive, Volume II, Radar Remote Sensing and Surface Scattering and Emission Theory*, ISBN 0-201-10760-0, Addison-Wesley, 1982

This page left intentionally blank.

Appendix C – Orbital SAR with Pulses in the Air

Herein we calculate the relationship of "sweet" orbital geometries to radar operating parameters, specifically constraints on PRF.

Consider the geometry of Figure C-1.
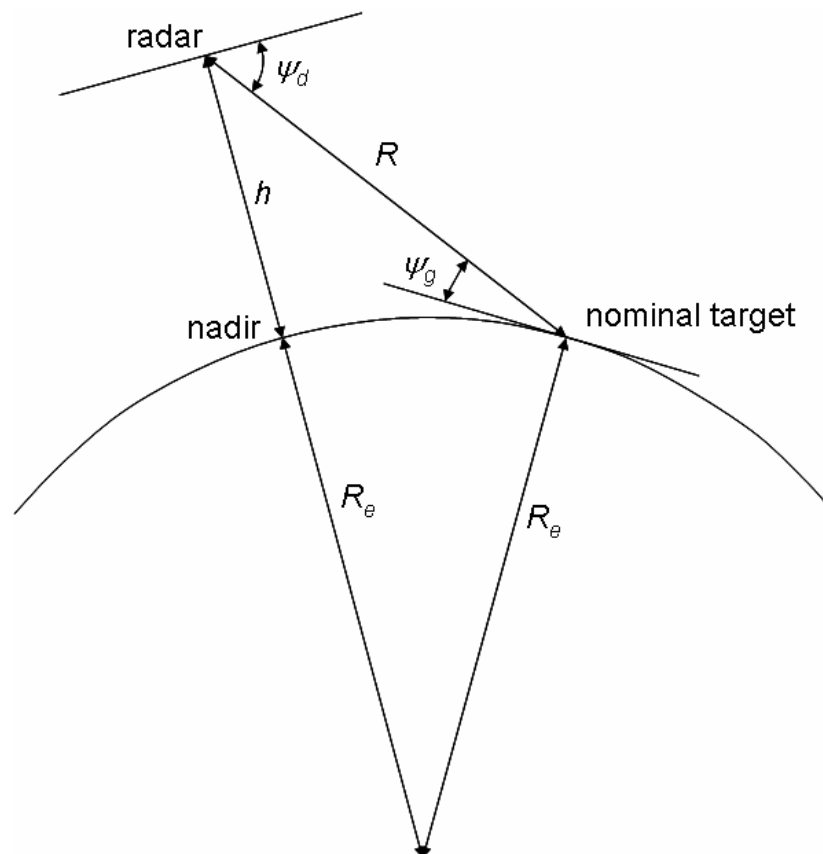
Figure C-1. Geometry definitions for orbital SAR.

We define

R = nominal range from radar to target scene,
R_e = radius of curvature of the surface,
h = nominal radar altitude,
ψ_g = nominal grazing angle at the target scene, and
ψ_d = nominal depression angle at the radar.   (C-1)

Note that the grazing angles are the complements of their corresponding incidence angles. We also note that useful values for R_e are

Table C-1. Nominal Equatorial Radius

Earth	6378.137 km
Moon	1738.1 km

From earlier in the main body of the report we recall that for nadir to be occluded or eclipsed by a transmitted pulse requires the geometric constraint

$$\frac{h}{R} = \frac{n_p}{m_p + 1/2} \tag{C-2}$$

for integer values of m_p and n_p, where

m_p = number of transmitted pulses 'in the air' between radar and target scene,
n_p = number of pulses 'in the air' between radar and nadir, $\hspace{2em}$ (C-3)

and recall that this requires $n_p \le m_p$.

From geometry, the target local nominal grazing angle on a curved surface is given by

$$\sin \psi_g = \frac{h}{R}\left(1 + \frac{h}{2R_e}\right) - \frac{R}{2R_e} \tag{C-4}$$

The depression angle from local horizontal at the radar is given by

$$\sin \psi_d = \frac{h}{R}\left(1 - \frac{h}{2(R_e + h)}\right) + \frac{R}{2(R_e + h)}. \tag{C-5}$$

These of course neglect any atmospheric refraction effects.

This allows us to calculate "sweet" grazing angles ψ_g for geometrical parameters m_p and n_p. However these will also vary with radar height h and surface curvature radius R_e.

Preferred Grazing Angle Tables

The following tables identify optimal, or sweet, target scene grazing angles for several earth and lunar orbiting geometries.

Table C-2. "Sweet" target scene grazing angles (degrees) for 50 km height above lunar surface.

		n = pulses for nadir									
		1.000	2.000	3.000	4.000	5.000	6.000	7.000	8.000	9.000	10.000
m = pulses in air roundtrip to target	1.000	40.895	N/A	N/A	N/A	N/A	N/A	N/A	N/A	N/A	N/A
	2.000	21.703	52.516	N/A	N/A	N/A	N/A	N/A	N/A	N/A	N/A
	3.000	13.856	33.675	58.506	N/A	N/A	N/A	N/A	N/A	N/A	N/A
	4.000	9.247	24.738	40.895	62.312	N/A	N/A	N/A	N/A	N/A	N/A
	5.000	6.046	19.227	31.798	45.886	65.005	N/A	N/A	N/A	N/A	N/A
	6.000	3.587	15.389	25.913	36.932	49.605	67.039	N/A	N/A	N/A	N/A
	7.000	1.569	12.507	21.703	30.933	40.895	52.516	68.646	N/A	N/A	N/A
	8.000	N/A	10.227	18.498	26.538	34.907	44.080	54.876	69.956	N/A	N/A
	9.000	N/A	8.351	15.949	23.138	30.435	38.162	46.712	56.839	71.052	N/A
	10.000	N/A	6.760	13.856	20.406	26.926	33.675	40.895	48.937	58.506	71.985

Table C-3. "Sweet" target scene grazing angles (degrees) for 100 km height above lunar surface.

		n = pulses for nadir									
		1.000	2.000	3.000	4.000	5.000	6.000	7.000	8.000	9.000	10.000
m = pulses in air roundtrip to target	1.000	39.993	N/A	N/A	N/A	N/A	N/A	N/A	N/A	N/A	N/A
	2.000	19.852	51.911	N/A	N/A	N/A	N/A	N/A	N/A	N/A	N/A
	3.000	11.142	32.515	58.021	N/A	N/A	N/A	N/A	N/A	N/A	N/A
	4.000	5.691	23.110	39.993	61.896	N/A	N/A	N/A	N/A	N/A	N/A
	5.000	1.652	17.157	30.558	45.124	64.635	N/A	N/A	N/A	N/A	N/A
	6.000	N/A	12.888	24.361	35.898	48.935	66.703	N/A	N/A	N/A	N/A
	7.000	N/A	9.582	19.852	29.652	39.993	51.911	68.335	N/A	N/A	N/A
	8.000	N/A	6.881	16.355	25.024	33.797	43.270	54.320	69.667	N/A	N/A
	9.000	N/A	4.585	13.520	21.398	29.130	37.171	45.972	56.322	70.779	N/A
	10.000	N/A	2.575	11.142	18.445	25.434	32.515	39.993	48.251	58.021	71.727

Table C-4. "Sweet" target scene grazing angles (degrees) for 150 km height above lunar surface.

		n = pulses for nadir									
		1.000	2.000	3.000	4.000	5.000	6.000	7.000	8.000	9.000	10.000
m = pulses in air roundtrip to target	1.000	39.102	N/A	N/A	N/A	N/A	N/A	N/A	N/A	N/A	N/A
	2.000	18.022	51.314	N/A	N/A	N/A	N/A	N/A	N/A	N/A	N/A
	3.000	8.454	31.371	57.542	N/A	N/A	N/A	N/A	N/A	N/A	N/A
	4.000	2.157	21.502	39.102	61.486	N/A	N/A	N/A	N/A	N/A	N/A
	5.000	N/A	15.109	29.333	44.373	64.270	N/A	N/A	N/A	N/A	N/A
	6.000	N/A	10.412	22.828	34.877	48.273	66.371	N/A	N/A	N/A	N/A
	7.000	N/A	6.682	18.022	28.388	39.102	51.314	68.029	N/A	N/A	N/A
	8.000	N/A	3.558	14.236	23.528	32.701	42.471	53.772	69.381	N/A	N/A
	9.000	N/A	0.839	11.115	19.678	27.842	36.193	45.241	55.812	70.510	N/A
	10.000	N/A	N/A	8.454	16.506	23.961	31.371	39.102	47.574	57.542	71.472

Table C-5. "Sweet" target scene grazing angles (degrees) for 200 km height above earth surface.

	n = pulses for nadir											
	1.000	2.000	3.000	4.000	5.000	6.000	7.000	8.000	9.000	10.000	11.000	12.000
1.000	40.814	N/A	N/A	N/A	N/A	N/A	N/A	N/A	N/A	N/A	N/A	N/A
2.000	21.535	52.462	N/A	N/A	N/A	N/A	N/A	N/A	N/A	N/A	N/A	N/A
3.000	13.610	33.570	58.462	N/A	N/A	N/A	N/A	N/A	N/A	N/A	N/A	N/A
4.000	8.926	24.591	40.814	62.275	N/A	N/A	N/A	N/A	N/A	N/A	N/A	N/A
5.000	5.649	19.040	31.686	45.817	64.972	N/A	N/A	N/A	N/A	N/A	N/A	N/A
6.000	3.115	15.163	25.773	36.838	49.544	67.009	N/A	N/A	N/A	N/A	N/A	N/A
7.000	1.022	12.243	21.535	30.817	40.814	52.462	68.618	N/A	N/A	N/A	N/A	N/A
8.000	N/A	9.924	18.304	26.401	34.806	44.006	54.826	69.930	N/A	N/A	N/A	N/A
9.000	N/A	8.010	15.729	22.980	30.317	38.072	46.645	56.792	71.027	N/A	N/A	N/A
10.000	N/A	6.382	13.610	20.229	26.791	33.570	40.814	48.875	58.462	71.962	N/A	N/A
11.000	N/A	4.962	11.821	17.951	23.925	29.991	36.333	43.159	50.791	59.902	72.771	N/A
12.000	N/A	3.699	10.279	16.023	21.535	27.056	32.737	38.722	45.195	52.462	61.161	73.480
13.000	N/A	2.559	8.926	14.361	19.502	24.591	29.763	35.129	40.814	46.986	53.935	62.275
14.000	N/A	1.514	7.722	12.906	17.744	22.482	27.248	32.138	37.240	42.667	48.577	55.247
15.000	N/A	0.547	6.637	11.616	16.203	20.650	25.086	29.594	34.246	39.122	44.324	50.003
16.000	N/A	N/A	5.649	10.460	14.835	19.040	23.200	27.394	31.686	36.135	40.814	45.817
17.000	N/A	N/A	4.741	9.414	13.610	17.608	21.535	25.468	29.463	33.570	37.842	42.346
18.000	N/A	N/A	3.900	8.458	12.503	16.324	20.052	23.763	27.509	31.333	35.278	39.394
19.000	N/A	N/A	3.115	7.580	11.495	15.163	18.719	22.239	25.773	29.359	33.035	36.838
20.000	N/A	N/A	2.378	6.767	10.570	14.105	17.512	20.866	24.217	27.601	31.050	34.594
21.000	N/A	N/A	1.682	6.009	9.717	13.136	16.411	19.621	22.812	26.021	29.275	32.602
22.000	N/A	N/A	1.022	5.300	8.926	12.243	15.402	18.484	21.535	24.591	27.677	30.817

m = pulses in air roundtrip to target

Table C-6. "Sweet" target scene grazing angles (degrees) for 400 km height above earth surface.

	n = pulses for nadir											
	1.000	2.000	3.000	4.000	5.000	6.000	7.000	8.000	9.000	10.000	11.000	12.000
1.000	39.832	N/A	N/A	N/A	N/A	N/A	N/A	N/A	N/A	N/A	N/A	N/A
2.000	19.521	51.803	N/A	N/A	N/A	N/A	N/A	N/A	N/A	N/A	N/A	N/A
3.000	10.657	32.308	57.934	N/A	N/A	N/A	N/A	N/A	N/A	N/A	N/A	N/A
4.000	5.053	22.819	39.832	61.822	N/A	N/A	N/A	N/A	N/A	N/A	N/A	N/A
5.000	0.863	16.787	30.336	44.988	64.569	N/A	N/A	N/A	N/A	N/A	N/A	N/A
6.000	N/A	12.441	24.084	35.713	48.815	66.643	N/A	N/A	N/A	N/A	N/A	N/A
7.000	N/A	9.058	19.521	29.424	39.832	51.803	68.280	N/A	N/A	N/A	N/A	N/A
8.000	N/A	6.281	15.972	24.753	33.599	43.125	54.221	69.615	N/A	N/A	N/A	N/A
9.000	N/A	3.910	13.085	21.087	28.897	36.994	45.840	56.230	70.730	N/A	N/A	N/A
10.000	N/A	1.824	10.657	18.095	25.168	32.308	39.832	48.128	57.934	71.681	N/A	N/A
11.000	N/A	N/A	8.560	15.580	22.104	28.555	35.188	42.252	50.093	59.403	72.503	N/A
12.000	N/A	N/A	6.712	13.417	19.521	25.450	31.437	37.667	44.349	51.803	60.687	73.224
13.000	N/A	N/A	5.053	11.523	17.297	22.819	28.314	33.936	39.832	46.190	53.310	61.822
14.000	N/A	N/A	3.545	9.837	15.349	20.548	25.654	30.810	36.131	41.745	47.823	54.651
15.000	N/A	N/A	2.155	8.317	13.620	18.556	23.350	28.136	33.014	38.082	43.452	49.285
16.000	N/A	N/A	0.863	6.931	12.067	16.787	21.323	25.809	30.336	34.982	39.832	44.988
17.000	N/A	N/A	N/A	5.656	10.657	15.198	19.521	23.759	27.998	32.308	36.755	41.413
18.000	N/A	N/A	N/A	4.472	9.365	13.757	17.901	21.930	25.931	29.966	34.091	38.363
19.000	N/A	N/A	N/A	3.365	8.173	12.441	16.432	20.285	24.084	27.889	31.749	35.713
20.000	N/A	N/A	N/A	2.323	7.064	11.229	15.090	18.792	22.418	26.029	29.668	33.377
21.000	N/A	N/A	N/A	1.337	6.028	10.105	13.856	17.427	20.905	24.348	27.800	31.296
22.000	N/A	N/A	N/A	0.399	5.053	9.058	12.713	16.171	19.521	22.819	26.109	29.424

m = pulses in air roundtrip to target

Table C-7. "Sweet" target scene grazing angles (degrees) for 600 km height above earth surface.

n = pulses for nadir

m = pulses in air roundtrip to target

	1.000	2.000	3.000	4.000	5.000	6.000	7.000	8.000	9.000	10.000	11.000	12.000
1.000	38.864	N/A	N/A	N/A	N/A	N/A	N/A	N/A	N/A	N/A	N/A	N/A
2.000	17.531	51.154	N/A	N/A	N/A	N/A	N/A	N/A	N/A	N/A	N/A	N/A
3.000	7.731	31.064	57.414	N/A	N/A	N/A	N/A	N/A	N/A	N/A	N/A	N/A
4.000	1.204	21.071	38.864	61.376	N/A	N/A	N/A	N/A	N/A	N/A	N/A	N/A
5.000	N/A	14.560	29.004	44.171	64.173	N/A	N/A	N/A	N/A	N/A	N/A	N/A
6.000	N/A	9.747	22.416	34.604	48.096	66.282	N/A	N/A	N/A	N/A	N/A	N/A
7.000	N/A	5.902	17.531	28.049	38.864	51.154	67.947	N/A	N/A	N/A	N/A	N/A
8.000	N/A	2.663	13.667	23.127	32.408	42.256	53.625	69.304	N/A	N/A	N/A	N/A
9.000	N/A	N/A	10.469	19.217	27.497	35.931	45.045	55.676	70.438	N/A	N/A	N/A
10.000	N/A	N/A	7.731	15.986	23.567	31.064	38.864	47.392	57.414	71.404	N/A	N/A
11.000	N/A	N/A	5.327	13.236	20.307	27.138	34.059	41.358	49.404	58.912	72.239	N/A
12.000	N/A	N/A	3.170	10.840	17.531	23.865	30.155	36.627	43.515	51.154	60.220	72.971
13.000	N/A	N/A	1.204	8.713	15.117	21.071	26.885	32.758	38.864	45.405	52.694	61.376
14.000	N/A	N/A	N/A	6.796	12.982	18.638	24.081	29.500	35.037	40.836	47.080	54.064
15.000	N/A	N/A	N/A	5.045	11.066	16.487	21.636	26.697	31.800	37.056	42.593	48.578
16.000	N/A	N/A	N/A	3.429	9.327	14.560	19.471	24.245	29.004	33.846	38.864	44.171
17.000	N/A	N/A	N/A	1.922	7.731	12.815	17.531	22.071	26.552	31.064	35.683	40.494
18.000	N/A	N/A	N/A	0.507	6.255	11.219	15.775	20.121	24.374	28.617	32.919	37.347
19.000	N/A	N/A	N/A	N/A	4.878	9.747	14.172	18.355	22.416	26.438	30.481	34.604
20.000	N/A	N/A	N/A	N/A	3.585	8.380	12.696	16.742	20.643	24.477	28.305	32.178
21.000	N/A	N/A	N/A	N/A	2.364	7.103	11.328	15.259	19.022	22.698	26.344	30.008
22.000	N/A	N/A	N/A	N/A	1.204	5.902	10.053	13.886	17.531	21.071	24.562	28.049

Table C-8. "Sweet" target scene grazing angles (degrees) for 800 km height above earth surface.

n = pulses for nadir

m = pulses in air roundtrip to target

	1.000	2.000	3.000	4.000	5.000	6.000	7.000	8.000	9.000	10.000	11.000	12.000
1.000	37.909	N/A	N/A	N/A	N/A	N/A	N/A	N/A	N/A	N/A	N/A	N/A
2.000	15.563	50.514	N/A	N/A	N/A	N/A	N/A	N/A	N/A	N/A	N/A	N/A
3.000	4.826	29.836	56.901	N/A	N/A	N/A	N/A	N/A	N/A	N/A	N/A	N/A
4.000	N/A	19.342	37.909	60.936	N/A	N/A	N/A	N/A	N/A	N/A	N/A	N/A
5.000	N/A	12.356	27.690	43.366	63.782	N/A	N/A	N/A	N/A	N/A	N/A	N/A
6.000	N/A	7.075	20.769	33.509	47.387	65.927	N/A	N/A	N/A	N/A	N/A	N/A
7.000	N/A	2.763	15.563	26.692	37.909	50.514	67.619	N/A	N/A	N/A	N/A	N/A
8.000	N/A	N/A	11.384	21.520	31.232	41.400	53.037	68.998	N/A	N/A	N/A	N/A
9.000	N/A	N/A	7.874	17.368	26.114	34.882	44.262	55.129	70.150	N/A	N/A	N/A
10.000	N/A	N/A	4.826	13.899	21.984	29.836	37.909	46.667	56.901	71.131	N/A	N/A
11.000	N/A	N/A	2.110	10.914	18.530	25.738	32.945	40.476	48.725	58.427	71.979	N/A
12.000	N/A	N/A	N/A	8.284	15.563	22.300	28.890	35.602	42.692	50.514	59.760	72.723
13.000	N/A	N/A	N/A	5.924	12.960	19.342	25.473	31.596	37.909	44.630	52.087	60.936
14.000	N/A	N/A	N/A	3.774	10.637	16.749	22.527	28.207	33.957	39.939	46.347	53.486
15.000	N/A	N/A	N/A	1.790	8.534	14.440	19.942	25.277	30.601	36.045	41.745	47.880
16.000	N/A	N/A	N/A	N/A	6.608	12.356	17.639	22.700	27.690	32.724	37.909	43.366
17.000	N/A	N/A	N/A	N/A	4.826	10.454	15.563	20.403	25.125	29.836	34.626	39.588
18.000	N/A	N/A	N/A	N/A	3.163	8.702	13.672	18.332	22.835	27.285	31.763	36.345
19.000	N/A	N/A	N/A	N/A	1.599	7.075	11.934	16.446	20.769	25.004	29.229	33.509
20.000	N/A	N/A	N/A	N/A	0.119	5.553	10.324	14.715	18.887	22.944	26.959	30.993
21.000	N/A	N/A	N/A	N/A	N/A	4.120	8.823	13.114	17.160	21.066	24.906	28.736
22.000	N/A	N/A	N/A	N/A	N/A	2.763	7.414	11.623	15.563	19.342	23.034	26.692

Typically for an orbital SAR, the radar height is dictated to the designer by other criteria. Consequently, we shall presume it as fixed. The task at hand is to select some optimized values of m_p and n_p, subject to the constraints above, which in turn defines a geometry and radar Pulse Repetition Frequency (PRF).

The following procedure can be used.

1. Calculate a minimum PRF due to Doppler considerations. This will be impacted by antenna size, and orbital velocity parameters. Scene size and ambiguity constraints will also play a role. A minimum PRF defines a maximum T_p.

2. From radar height h and a maximum T_p, a minimum index n_p can be calculated.

3. From the tables, select a suitable nominal grazing angle from columns for which n_p is greater than or equal to the previously calculated minimum value. The selected grazing angle will define indices m_p and n_p, which in turn can be used to calculate the actual values for the remaining geometric parameters and PRF. Note that too large an n_p will result in limiting swath and potential range ambiguities.

4. Radar pulse width can now be adjusted to maximize duty factor subject to these and other radar timing parameters.

This procedure should allow maximizing the radar duty factor.

Example – Lunar Orbiting SAR

Consider a SAR in a circular lunar orbit at 100 km above the lunar surface. The desired grazing angles within the image are between 35 and 55 degrees, and the desired resolution is 100 m on the ground, with multilook. We presume an antenna azimuth aperture width of approximately 1.8 m with some aperture weighting, which allows approximately 2 kHz of Doppler bandwidth within the nominal antenna beam. With respect to the steps above:

1. If we choose a Doppler oversampling factor of approximately 1.4, then this corresponds to a minimum PRF of 2.8 kHz.

2. The radar height with this lower bound on PRF constrains $n_p \geq 2$.

3. From Table 3, we select $m_p=2$ and $n_p=2$, to allow a surface grazing angle of 51.9 degrees at the nominal range. Note that any range swath will cause near edge and far edge of the swath to deviate from this grazing angle somewhat. For example, a 15 km swath will have target scene grazing angles vary between 49.1 and 55 degrees. Another advantage of grazing angles at the steeper end of allowable values is the corresponding reduced range, leading to increased SNR, or alternatively lesser transmitter power required.

4. The corresponding radar PRF is very nearly 3 kHz. Allowing for some timing margins, this geometry with a 15 km swath will allow transmitted pulse widths of slightly more than 130 µs. These values in turn correspond to a transmitter duty factor of a not-to-shabby 39%.

Altitude Variations

To maintain nadir occlusion with $m_p=n_p=2$, the PRF needs to vary inversely with radar height h. Therefore, as height increases the PRF needs to decrease in inverse proportion, but Doppler bandwidth will not decrease. Consequently the Doppler oversampling factor will decrease in inverse proportion to height, yielding an increase in azimuth ambiguity. The tolerance to an increase in azimuth ambiguity at the maximum height needs to be judged. It may be as simple as reducing the desired azimuth scene width. Alternatively, we might consider parameters corresponding to some $n_p>2$, but a quick analysis shows rather limited potential for our example.

With a substantial height decrease, the radar may consider shifting to parameters corresponding to $m_p=n_p=1$.

Using a Smaller Antenna

Decreasing the azimuth length of the antenna will increase the Doppler bandwidth within the antenna beam. However if the PRF is fixed due to the constraints of nadir occlusion, then the Doppler oversampling factor will decrease in inverse proportion to antenna length, yielding an increase in azimuth ambiguity. As with altitude variations, the increase in azimuth ambiguity needs to be evaluated and judged, with perhaps adjustments made to acceptable-quality azimuth scene widths. Also as with altitude variations, we might generally consider parameters corresponding to some $n_p>2$, but with the same limited potential previously mentioned for our particular example.

Increasing the azimuth length of the antenna advantageously reduces azimuth ambiguity, but will further constrain the illuminated scene.

Summary

We emphasize the following points:

- Orbital SAR systems must necessarily operate at long range and high velocity. This typically results in the need for "pulses in the air", with the deleterious effect of needing to deal with a bright nadir return.

- Flexibility in allowed imaging geometry and radar PRF enables occluding the nadir return with a transmitted pulse.

- Occluding the nadir return with a transmitted pulse maximizing radar duty factor and achievable swath width. This represents a "sweet spot" in radar parameters.

Distribution

Unlimited Release

1	MS 1330	A. W. Doerry	5342
1	MS 1330	W. H. Hensley	5342
1	MS 1330	B. L. Remund	5340
1	MS 1330	B. L. Burns	5340
1	MS 1330	D. F. Dubbert	5345
1	MS 1330	G. R. Sloan	5345
1	MS 0537	D. L. Bickel	5354
1	MS 0537	J. T. Cordaro	5354
2	MS 9018	Central Technical Files	8945-1
2	MS 0899	Technical Library	4536

;-)